Chapter 3

Habitat determinants of primary production in the sea

In the trophic–dynamic approach to ecosystems, we try to measure the production at each link in the food chain or web, at each trophic level. "Production" is incorporation of new organic matter into cellular material, that is, an increase in biomass. For phytoplankton, this is done by photosynthesis, the dominant type of *primary production*. (Chemosynthesis is important in some environments.) *Gross* primary production is total photosynthate generated, and *net* primary production (i.e. growth) is gross production less respiration. Net production is available to herbivores. For herbivores, an increase in biomass can be expressed as a difference:

$$\text{secondary production} = \text{phytoplankton eaten} - \text{feces} - \text{respiration}$$

As will be shown eventually, secondary and higher-level rates are much harder to measure than primary productivity. Production *rates* (biomass elaborated per unit time) are often termed *productivities*. Oceanographers speak of "the primary productivity", meaning the rate of phytoplankton production, usually measured as carbon newly incorporated in organic matter per unit area (or volume) per unit time.

The light-dependent reactions of photosynthesis (Fig. 3.1) comprise absorption of light energy; transfer of electrons through the photosynthetic reaction centers coupled with reduction of water to oxygen and production of adenosine triphosphate (ATP) and the reduced form of nicotinamide adenine dinucleotide phosphate (NADPH). The NADPH produced is then used as reducing power for the biosynthetic reactions in the Calvin cycle of photosynthesis. The light-independent reactions (formerly called "dark" reactions) of photosynthesis fix CO_2 into carbohydrates. Thus, photosynthesis is often described in terms of the biochemical elaboration of carbohydrate (sugars and their polymers). We will follow that tradition, but keep in mind that most unicellular algae direct more than half of their reduced carbon to protein synthesis, and that the principal store of high-energy molecules is often lipid. The overall photosynthetic reaction producing carbohydrates is:

$$2H_2O^* + CO_2 + \text{light} \xrightarrow{\text{Chl-}a} CH_2O + H_2O + O_2^*$$

The asterisks indicate that the oxygen produced is from the water reactant, not from the carbon dioxide. The water on the product side derives from a dehydroxylation step. This generalized reaction has two components, the light reactions of photosystem II (PSII) and photosystem I (PSI):

$$2H_2O^* + \text{light} \xrightarrow{\text{PSII}} 4H^+ + 4e^- + O_2^*$$

$$NADP^+ + H^+ + 2e^- \xrightarrow{\text{PSI}} NADPH$$

and the light-independent reaction:

$$CO_2 + 4\,H^+ + 4\,e^- \xrightarrow{\text{RuBisCO}} CH_2O + H_2O$$

where the free energy of cleavage of high-energy phosphate bonds of ATP and the reducing power of NADPH are used to fix and reduce CO_2 to form carbohydrate. This reaction is mediated by the enzyme ribulose bis-phosphate carboxylase (RuBisCO).

The pigment system (considered in Chapter 2) gives the phytoplankton cell access to energy from most of the visible spectrum. An example of the relative roles of different pigments in absorbing light is shown in Fig. 3.2a.

Biological Oceanography, Second Edition. Charles B. Miller, Patricia A. Wheeler.

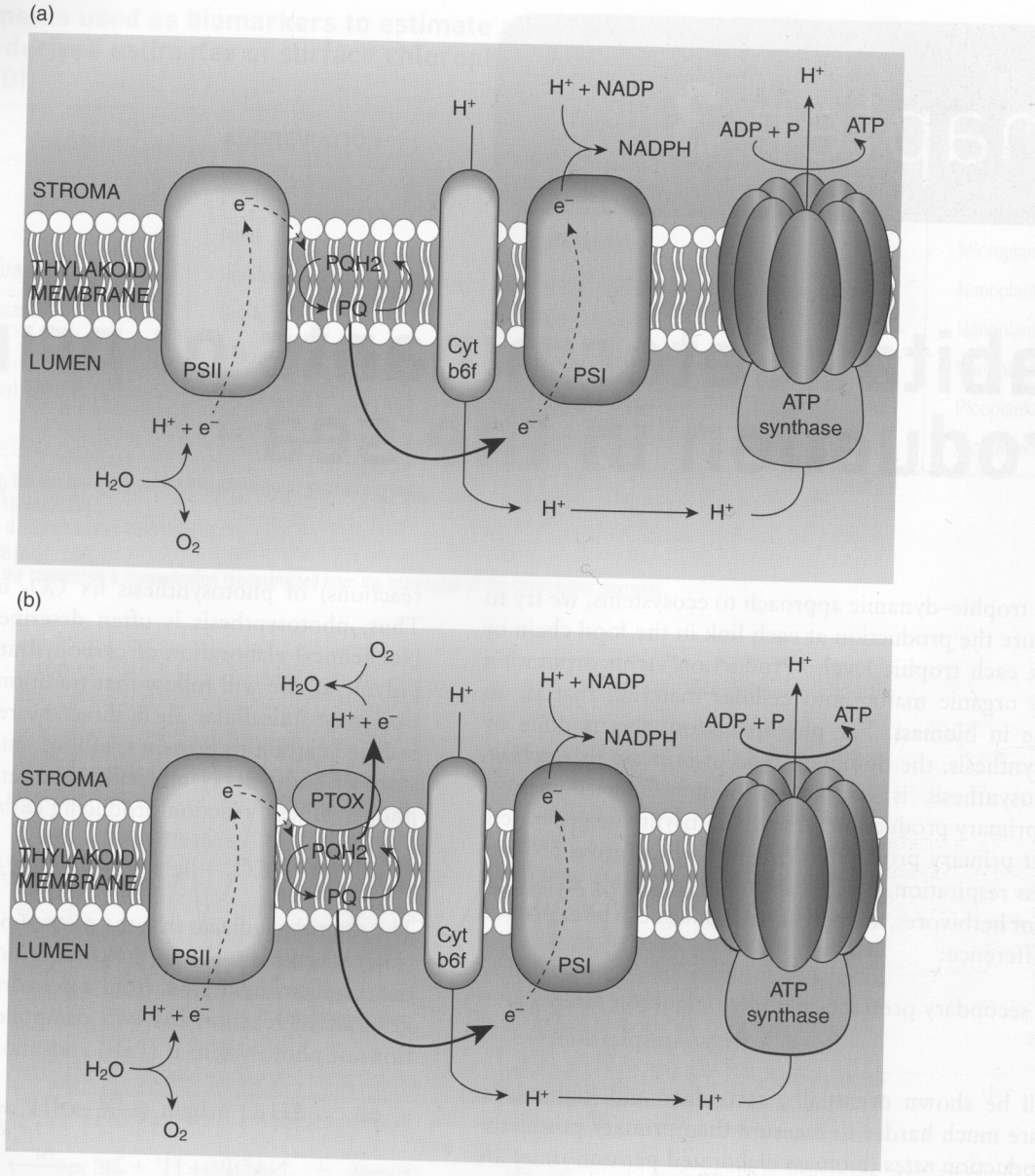

Fig. 3.1 Principal components and electron-flow pathways for the light reactions of photosynthesis. (a) Linear electron flow begins with excitation of the photosynthetic reaction centers, PSII and PSI, and with splitting of water by the oxygen-evolving complex of PSII. Electrons are passed from PSII to the plastoquinone (PQ) pool and then to PSI, where NADPH is formed. The cytochrome complex (cyt b_6f) pumps in protons that drive ATP production. (b) Under conditions of high light and low nutrients, plastoquinol terminal oxidase (PTOX) is activated and serves as an electron relief valve that uses excess electrons to reduce O_2 to water, so that less NADPH is formed than during linear electron transport. (After Zehr & Kudela 2009.)

Absorption by pigments is not 100% perfect, and some wavelengths are more effective than others at driving photosynthesis. This is shown in the "action spectrum" for photosynthesis (Fig. 3.2b). The highest overall effectiveness is found at those wavelengths centered at 465 nm, which are dominant in deeper ocean layers. This is true for phytoplankton generally. Lewis *et al.* (1985) have shown this by producing action spectra for natural phytoplankton assemblages at various ocean sites. All have their peak at 425–450 nm, a broad shoulder to 550 nm, and a rise at 675 nm (Fig. 3.3). Photosynthetic yield per quantum drops off rapidly below 425 nm and has low values from 600 to 650 nm – wavelengths not important in pelagic habitats except at the very surface.

There is a remarkable triple complementarity among the spectra of sunlight, the light transmissivity of water, and the absorption bands of various algal pigments. Absorption of light by water has a minimum with respect to wavelength, a window of clarity (Yentsch 1980), right at the peak range of wavelengths of solar irradiance (Fig. 1.5),

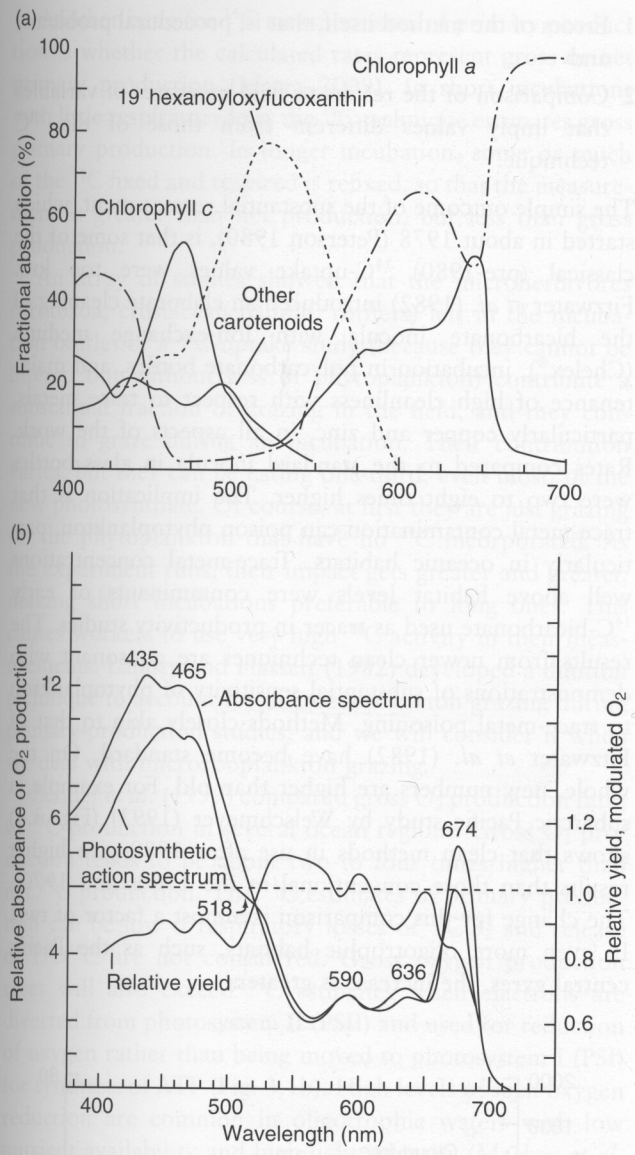

Fig. 3.2 (a) Fractional contribution to absorption of light by different pigments in live *Emiliania huxleyi*, a coccolithophorid. Contributions to absorbance add to 100% at each wavelength. Pigments are chlorophyll-*a*, chlorophyll-*c*, 19′ hexanoyloxyfucoxanthin, and other carotenoids. (b) Absorbance spectrum and photosynthetic action spectrum of oxygen production per quantum in *E. huxleyi*. The ratio [photosynthesis/absorbance], the relative yield, shows that absorbed quanta at all wavelengths are roughly equally effective. (After Haxo 1985.)

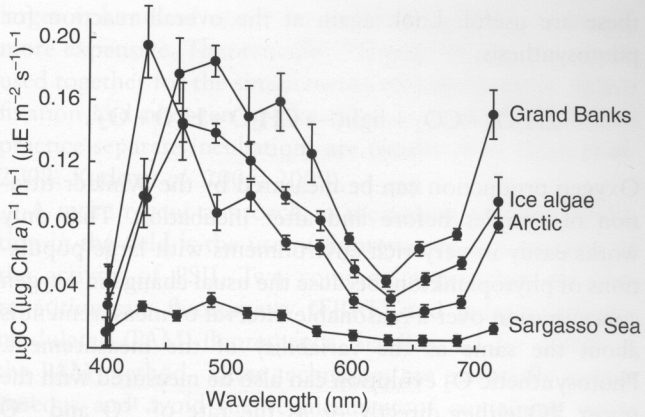

Fig. 3.3 Photosynthetic action spectra for natural phytoplankton assemblages from four regions: Grand Banks (showing ± 1 Standard Error), ice algae, Arctic open water, and Sargasso Sea. (After Lewis *et al.* 1985.)

the wavelengths of visible and photosynthetically active light. The absorption peaks of phytoplankton pigments (Fig. 3.2b) tend to be centered over the deep trough in the absorption coefficient, k, spectrum of water (Fig. 1.5b). Most importantly, the absorbance peak for "antenna pigments" and chlorophyll-*a* acting together centers close to the deepest trough near 465 nm. This is not an accidental coincidence, but represents tuning by natural selection of the photosynthetic system to the properties of water.

The factors that control the overall rates of photosynthesis, primary productivity, in the sea are: (i) those that control the rates of reaction of the photosystems (PSI and PSII), and (ii) those that control the rates of the light-independent reactions. The former are light intensity and availability of water and carbon dioxide. Water and carbon dioxide are in abundant supply in seawater, although reaction rates can be forced somewhat by carbon dioxide loading. The latter include temperature and availability of *nutrients*. Nutrients are "fixed" nitrogen, phosphate, various metal ions, silicic acid (for diatoms and chrysophytes), and sometimes vitamins. Roles of a number of these are considered here.

Estimation of primary production

Measurement of productivity is most successfully done at the primary-producer level in pelagic habitats, because in some cases it is easy to separate phytoplankton from their herbivores and observe the rate of accumulation of phytoplankton cells. We have a number of methods that are simple in principle, more complex in practice. The basic method is to collect a bottle of seawater from a place and depth to be studied, check that no herbivores are present (use a coarse filter perhaps), and measure the increase in phytoplankton biomass during some time interval. This would most appropriately be the period of the natural illumination cycle, 24 hours, but adverse responses of the phytoplankton to confinement often force shorter incubations. Alternately, *any* photosynthetic product can be measured or the reduction of *any* photosynthetic resource can be determined. In practice only a few of

these are useful. Look again at the overall reaction for photosynthesis:

$$2H_2O^* + CO_2 + \text{light} \rightarrow CH_2O + H_2O + O_2^*.$$

Oxygen production can be measured by the Winkler titration of samples before and after incubation. That only works easily in very rich environments with large populations of phytoplankton, because the usual change in oxygen concentration over a reasonable interval of measurement is about the same as the variability of the measurement. Photosynthetic O_2 evolution can also be measured with the tracer ^{18}O either directly or as the rate of ^{18}O and ^{16}O evolution from a mixture of $H_2{}^{18}O$ and $H_2{}^{16}O$ (Bender *et al.* 1987).

A long-favored method is the carbon-14 incorporation technique first introduced to ecology by Steeman-Nielsen (1952). A bottle of seawater, to which ^{14}C as sodium bicarbonate has been added, is incubated at its depth of collection in the sea (or more often in a simulated photic and thermal environment on deck). After an interval, the bottle is retrieved, the phytoplankton are filtered off, and the amount of ^{14}C incorporated in them is measured by scintillation counting. The net (since respiration goes on throughout the incubation as well as photosynthesis) primary production is obtained by multiplying the fraction of the ^{14}C taken up (e.g. counts per minute in filtered cells/counts per minute provided) by total carbonate in the bottle. Thus, a carbonate determination is required as well. The standard recipe for ^{14}C-uptake production measurement is given by Parsons *et al.* (1984). They give the following final equation for the calculation of the result:

$$\text{Photosynthesis (mg C m}^{-3}\text{ h}^{-1}) = [(R_s - R_b)W]/RT \qquad \text{(Eqn. 3.1)}$$

where R is the counting rate to be expected for the entire addition of ^{14}C; R_s and R_b are counting rates for the filtered sample and a blank, respectively; W is the total weight of carbonate carbon in the water ($mg\,C\,m^{-3}$); and T is the duration of the incubation in hours. A dark-bottle uptake experiment is usually included in the observational design to account for carbon-isotope exchange processes other than those of primary production *per se*. Note that the volume of the incubation container is implicit in all of R_s, R_b, and R (say, ^{14}C counts per liter), so it cancels.

The ^{14}C method has been used all over the world since 1952. There is a large mass of data, and much of what we know about the vertical and geographical distribution of primary productivity comes from it. However, it has always been recognized that the method has some uncertainties associated with it, and during the 1980s even the general levels measured were questioned. The recognized problems fall into two classes:

1 Errors of the method itself, that is, procedural problems; and
2 Comparison of the results to field measures of variables that imply values different from those of the ^{14}C technique.

The simple outcome of the substantial reassessment, which started in about 1978 (Peterson 1980), is that some of the classical (pre-1980) ^{14}C-uptake values were too low. Fitzwater *et al.* (1982) introduced an elaborate cleaning of the bicarbonate inocula with ion-exchange medium (Chelex®), incubation in polycarbonate bottles, and maintenance of high cleanliness with respect to trace metals, particularly copper and zinc, in all aspects of the work. Rates compared to the standard inocula in glass bottles were two to eight times higher. The implication is that trace-metal contamination can poison phytoplankton, particularly in oceanic habitats. Trace-metal concentrations well above habitat levels were contaminants of early ^{14}C-bicarbonate used as tracer in productivity studies. The results from newer clean techniques are consonant with demonstrations of substantial sensitivity of phytoplankton to trace-metal poisoning. Methods closely akin to that of Fitzwater *et al.* (1982) have become standard. On the whole, new numbers are higher than old. For example, a subarctic Pacific study by Welschmeyer (1993) (Fig. 3.4) shows that clean methods in use after 1980 give higher results than those conventional in the 1960s and 1970s. The change for this comparison is almost a factor of two. In even more oligotrophic habitats, such as the Pacific central gyres, the increase is greater.

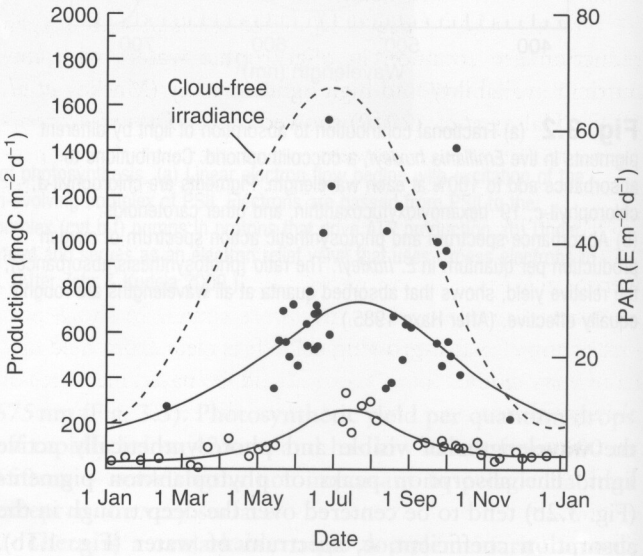

Fig. 3.4 Depth-integrated primary productivity in the subarctic Pacific compared to a generalized curve of PAR ("photosynthetically active radiation"). Filled circles are modern ^{14}C-uptake data from a trace-metal clean technique (1984–1988); open circles are data collected before 1980 with the then-standard ^{14}C-uptake method. (After Welschmeyer 1993.)

Another issue for ^{14}C measurements of primary production is whether the calculated rates represent gross or net primary production (Marra 2009). In short incubations with little respiratory loss, the ^{14}C technique estimates gross primary production. In longer incubation, some or much of the ^{14}C fixed and respired is refixed, so that the measurement is greater than net production, but less than gross production.

An array of studies showed that the microherbivores (protozoa, crustacean nauplii, rotifers) left in the incubation bottles of a ^{14}C-uptake study (because they cannot be filtered out without loss of phytoplankton) contribute a substantial fraction of grazing in the field, and they continue to graze during an incubation. Their contribution varies, but they can be eating one-third, even most, of the new photosynthate. Of course, at first they are just grazing on the phytoplankton that have no ^{14}C incorporated. As the experiment runs, their impact gets greater and greater, making short incubations preferable to long ones. This causes workers to use very high ^{14}C activity in their measurements. Landry and Hassett (1982) developed a dilution technique to account for microzooplankton grazing during primary-production studies, and we will consider it when we deal with microzooplankton grazing.

Bender *et al.* (1999) compared gross O_2 production rates to ^{14}C production in several ocean regions. Gross O_2 production tends to be about two to four times higher than net ^{14}C production. The ^{14}C estimates of primary production can be low if respiratory losses of $^{14}CO_2$ and release of $DO^{14}C$ are not considered. Gross oxygen production rates will also exceed ^{14}C estimates when electrons are diverted from photosystem II (PSII) and used for reduction of oxygen rather than being moved to photosystem I (PSI) for synthesis of ATP (Fig. 3.1b). High levels of such oxygen reduction are common in oligotrophic waters with low nutrient availability and high light intensity (Mackey *et al.* 2008). Halsey *et al.* (2010) showed that in *Dunaliella tertiolecta* the difference between net and gross primary production and the allocation of carbon to different metabolites depended on the growth rate. They found that in slow-growing cells gross O_2 production and gross C-fixation were much greater than net production rates. Conversely, gross and net production rates were similar in short-term incubations for fast-growing cells. It is clear from field and laboratory studies that ^{14}C-based and O_2-based measures of photosynthetic activity measure different component processes.

The stable isotope ^{13}C can also be used to measure rates of photosynthesis when use of radioisotopes is impractical (Hama *et al.* 1983). Bicarbonate enriched with ^{13}C is added to seawater, and the incorporation of CO_2 into particulate carbon (PC) is followed by measuring changes in the $^{13}C:^{12}C$ ratio of PC relative to the total CO_2 pool. The isotope ratio is usually measured by mass spectrometry. This method is less sensitive than the ^{14}C method; requires larger volumes of water for incubation; and is generally more expensive. Theoretically, ^{13}C and ^{15}N isotopes can be used together for the simultaneous measurement of carbon fixation and nitrogen uptake (Slawyk *et al.* 1977), but in practice separate incubations are usually done (Imai *et al.* 2002; Kudo *et al.* 2005, 2009).

A more recent approach to measuring primary produtions in the field is the use of fluorescence as a measure of the activity of PSII. Two common approaches are fast-repetition-rate fluorometry (FRRF) and pulse-amplitude-modulated (PAM) fluorescence. See Box 3.1 for details of the PAM method. These techniques are essentially instantaneous and avoid the requirement of containing water samples in incubation bottles. Cermeno *et al.* (2005) and Corno *et al.* (2006) found poor correspondence between near-surface (5 m) measurements of ^{14}C production and FRRF, but good correspondence between those measurements throughout the rest of the water column. Suggett *et al.* (2009) compared FRRF, ^{18}O production, and ^{14}C measurements. Their FRRF rates exceeded $^{14}CO_2$ uptake by a factor of five to 10. Suggett *et al.* attributed the difference to the uncoupling of electron flow between PSII and PSI and stressed that use of FRRF to examine aquatic productivity needs to focus on "a systematic description of how electrons are coupled to C fixation in nature". In conclusion, the ^{14}C technique is still the "standard" measurement for primary production in the sea, and measures something between net and gross carbon fixation by phytoplankton. Other approaches are being developed, but most are based on the light reactions of photosynthesis; the exact relationship between total light energy captured during photosynthesis and net or gross carbon fixation remains to be determined.

We will return later to the measurement of primary productivity. We will compare rates in different ocean areas, try to explain the differences, sum up the global total and try to fit the oceans into the overall biogeochemical cycling of carbon. But, now we turn to the factors affecting the rates.

Effects of light intensity (also called irradiance, illumination, and photon flux)

The photosynthetic rate varies over the entire range of light intensity from darkness (negative net productivity due to respiration) to full sunlight at the sea surface (considerable "photoinhibition"). The relationship is called a photosynthesis vs. irradiance (*P* vs. *E* curve), where *E* refers to the flux of radiant energy in units of mol quanta $m^{-2} s^{-1}$ (Fig. 3.5). The symbol "*I*" used in older texts to denote

Box 3.1 Use of chlorophyll fluorescence to measure photosynthetic activity

Light energy absorbed by chlorophyll can be directed in three ways: energizing photosynthesis (photochemistry); dissipation as heat; or re-emission as fluorescence. Photochemistry includes the activity of PSI, PSII and the assimilation of carbon. The spectrum of emitted fluorescence has a peak at a longer wavelength than the absorbed light. To measure emitted fluorescence, a light source is switched on and off at high frequency and the detector is tuned to detect only fluorescence excited by the stimulating light.

Pulse-amplitude-modulated (PAM) fluorometers and fast-repetition-rate fluorometers (FRRF) are both used to measure the photosynthetic activity of phytoplankton and cyanobacteria. We provide a simplified explanation of PAM fluorometry here (Mackey *et al.* 2008) and refer the reader to Kolber *et al.* (1998) and Suggett *et al.* (2009) for details of the FRRF technique. Variable fluorescence (F_v from Box Fig. 3.1.1) is the maximum fluorescence to bright flashes of dark-adapted cells minus the fluorescence to standardized dim flashes, $F_v = (F_m - F_o)$. F_v provides an estimate of the maximum potential rate of electron transport through PSII for dark-adapted cells. The maximum *potential* relative photosynthetic efficiency is proportional to F_v. The relative fluorescence decreases with continuing exposure to light and reaches an asymptote (F_s) after about 5 minutes. Fluorescence emission (F_s) is smaller because some of the electron acceptors are reduced and no longer able to accept electrons. The fluorescence response of light-adapted cells to a saturating flash is F_m'. The *actual* relative photosynthetic efficiency of PSII in the light-adapted state is $(F_m' - F_s)/F_m'$, a ratio called Φ_{PSII}. Multiplying Φ_{PSII} by the intensity of photosynthetically effective light, I_A, provides a measure of the PSII electron transport rate at that intensity. Thus, $\Phi_{PSII} \cdot I_A$ is an estimate of gross photosynthetic oxygen production. See Mackey *et al.* (2008) for thorough derivation of those relationships.

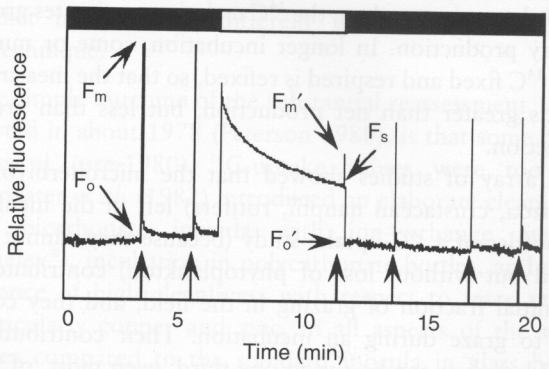

Box Fig. 3.1.1 The bar along the top shows periods of dark (black) and actinic light (white). Minimum fluorescence values (F_o and F_o') are determined using a low-intensity measuring light prior to delivery of the saturating light pulses. Arrows indicate the timing of saturating (3000 μmol quanta $m^{-2}s^{-1}$) actinic light pulses of 0.8 s duration. (After Mackey *et al.* 2008.)

PAM fluorometers generate data for F_o, F_m, F_s, F_o', and F_m' by the flashing and 'actinic' interval shown in Box Fig. 3.1.1. FRRF systems work on different principles, but are fast enough to generate roughly similar estimates as water column profiles. Both allow much higher spatial and temporal resolution of photosynthetic activity than is possible with the traditional ^{14}C technique. The fluorometric measures, however, have limited ecological relevance unless they can be converted to rates of carbon assimilation. When PSII, PSI and carbon assimilation activity are closely coupled, the fluorometric and ^{14}C measures give similar estimates of the rate of photosynthesis. However, the component photosynthetic processes are not always closely coupled, and that is a constraint for using PAM and FRRF for ecological studies. Some specific comparisons are described in the text.

irradiance is currently used to denote radiation intensity, which is the flux of radiant energy from a specified direction. The zero value of the photosynthetic rate scale cannot actually be at $E = 0$. Net photosynthesis is the result of "gross" photosynthesis minus respiration, which must have some small, positive value. The light intensity at which (Gross *PS* – Respiration) = 0.0 is termed the *compensation intensity*. However, in many regions (e.g. Fig. 3.5) the sensitivity to available light is so great that the positive intercept on the irradiance axis is not evident in the data. The response of the light-dependent (light-limited) portion of the relationship is linear and is represented by the initial slope, dP/dE, often symbolized as α. At higher intensities, such that a great portion of the chlorophyll is at all times in an excited state, the processes limiting the overall rate are the light-independent reactions. Thus, the photosystems are light saturated, and no further increase in rate occurs in response to greater intensity. The *P* vs. *E* curve becomes horizontal.

At even higher intensities, the rate begins to fall off, an effect called *photoinhibition*. This effect has different causes in different phytoplankton. One important cause is "photorespiration". The intermediate products of the light-independent reactions include five-carbon, phosphate-

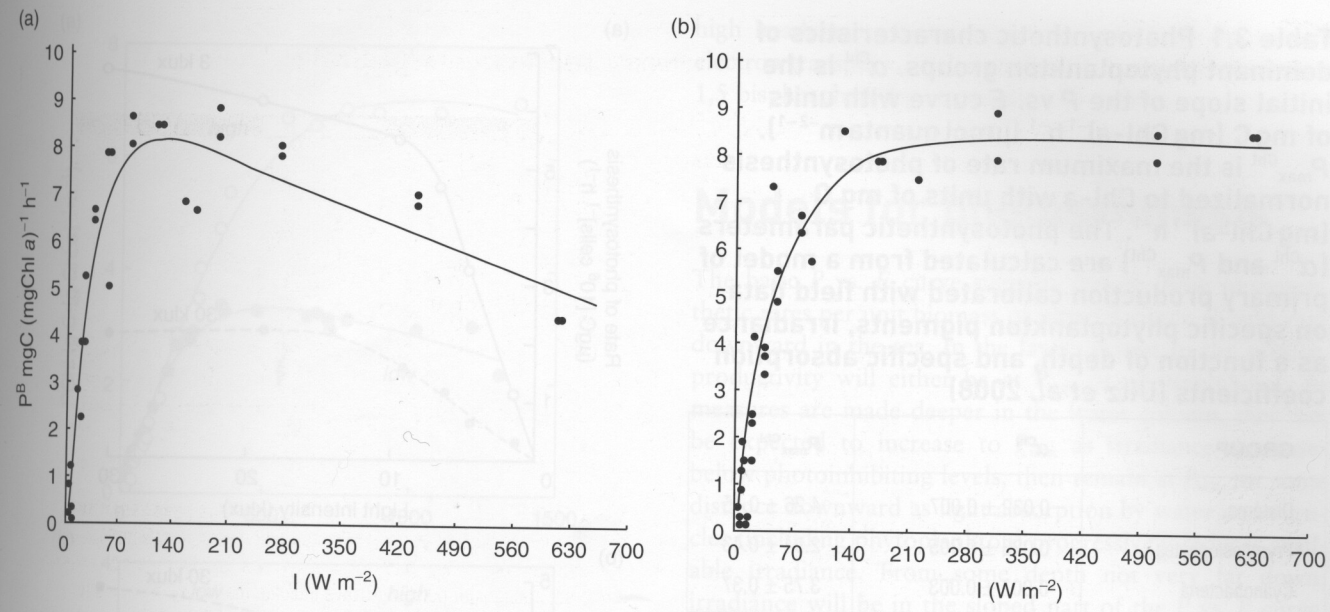

Fig. 3.5 Photosynthesis (per unit chlorophyll) vs. irradiance (*P* vs. *E*) curves developed in deck incubators for two different field situations: (a) a dense (13 mg Chl m^{-3}) diatom assemblage off Peru, exhibiting some photoinhibition; and (b) a predominantly flagellate assemblage of low density (0.3 mg Chl m^{-3}) off Nova Scotia with no evident photoinhibition (2 W m^{-2} = 10 μmol photons m^{-2} s^{-1}). (After Platt *et al.* 1980.)

esterified sugars, which are photolabile. Under intense light they break down into phosphoglycolic acid (C_2) and phosphoglyceric acid (C_3). The former is either excreted from the cell or metabolized to CO_2, but it cannot be returned to the photosynthetic pathway. The increase of this process (and probably other similar ones) reduces the overall rate of net photosynthesis.

Light-intensity response curves ("*P* vs. *E* curves") are all of this basic form, but differ in initial slope (α), maximum rate ("P_{max}"), intensity at onset of photoinhibition, and rate of decrease due to photoinhibition. When photosynthetic rates are normalized to (i.e., divided by) the levels of chlorophyll or cell carbon, the initial slope and maximum rates are denoted as α^B and $P_{max}{}^B$, where *B* denotes the normalization parameter used. The intersection of the initial slope of the *P* vs. *E* curve with P_{max} is K_E, the light-saturation parameter that indicates the irradiance where the shift in the controlling factor changes. Light responses may differ between clones of the same species cultured from different (or even the same!) habitats; between samples from different depths at the same station; and they differ substantially depending upon the history of light exposure of the phytoplankton. Various functional forms have been suggested to describe the *P* vs. *E* relationship. Several equations suggested by Platt and others are widely used. Platt and Jassby (1976) suggested a hyperbolic tangent function, $P = P_{max} \tanh(\alpha E/P_{max})$, which works well when photoinhibition is not obvious at higher intensities. This hyperbolic tangent function also has some theoretical attractions. Platt *et al.* (1980) fitted an array of *P* vs. *E* data for natural phytoplankton assemblages that did exhibit photoinhibition with the function:

$$P = P_{max}[1 - \exp^{(-\alpha E/P\,max)}][\exp^{(-\beta E/P\,max)}],$$

that has been applied by many field workers (e.g. Welschmeyer 1993). The parameter β is the intensity at onset of photoinhibition. This function applies to "normalized" photosynthetic rates, that is, rates per unit phytoplankton biomass. In fieldwork, the usual normalizing variable is chlorophyll-*a* concentration, and the ratio of the photosynthetic rate (carbon uptake) per unit volume to chlorophyll concentration is termed an *assimilation number*.

Different algal groups have significantly different light requirements for growth and photosynthesis (Richardson *et al.* 1983). Dinoflagellates and cyanobacteria photosynthesize and grow best at low light intensities. Diatoms can utilize low light intensities, but are much more tolerant of high light than most other groups. There are numerous reports and summaries of the photosynthetic parameters for *P* vs. *E* curves for most algal groups and many species of phytoplankton. We show some representative parameters in Table 3.1. Diatoms have the highest maximum rate of photosynthesis per unit chlorophyll ($P_{max}{}^{Chl}$), cyanobacteria are intermediate and the nanoflagellates (primarily prymnesiophytes) have the lowest $P_{max}{}^{Chl}$. Diatoms have the steepest initial slope for the rate of photosynthesis per unit chlorophyll (α^{Chl}), nanoflagellates have an intermediate slope, and cyanobacteria have the lowest slope.

In addition to genotypic differences, termed *photoadaptation*, in the ability of phytoplankton to utilize light, all phytoplankton exhibit short-term phenotypic adjustments, termed *photoacclimation*, in response to variations in light intensity (MacIntyre *et al.* 2002). The amount of

Table 3.1 Photosynthetic characteristics of dominant phytoplankton groups. α^{Chl} is the initial slope of the *P* vs. *E* curve with units of mg C (mg Chl-*a*)$^{-1}$ h^{-1} (μmol quanta m^{-2-1}). $P_{max}{}^{Chl}$ is the maximum rate of photosynthesis normalized to Chl-*a* with units of mg C (mg Chl-*a*)$^{-1}$ h^{-1}. The photosynthetic parameters (α^{Chl} and $P_{max}{}^{Chl}$) are calculated from a model of primary production calibrated with field data on specific phytoplankton pigments, irradiance as a function of depth, and specific absorption coefficients (Uitz *et al.* 2008)

GROUP	α^{Chl}	$P_{max}{}^{Chl}$
Diatoms	0.032 ± 0.007	4.26 ± 0.45
Prymnesiophytes	0.026 ± 0.005	2.94 ± 0.43
Cyanobacteria	0.007 ± 0.003	3.75 ± 0.37

photosynthetically active pigment may increase at low intensities (more chlorophyll-*a*, more P700 in the *Chlamydomonas* and *Phaeodactylum*, causing an increase in the slope of the *P* vs. *I* curves in short-term measurements (Fig. 3.6 a & c). Or the activity of the dark-reaction system may be increased at high light intensities (driven by increased availability of light-energized reactants – ATP, NADPH), causing the P_{max} value to rise in short-term comparisons for *Cyclotella* (Fig. 3.6b).

Figure 3.7 shows *P* vs. *E* curves for low- and high-light acclimated *Skeletonema costatum*. Interpretation of the curve depends on the variable to which photosynthesis is normalized. When photosynthesis is normalized to Chl-*a* (Fig. 3.7a), low- and high-light-acclimated cells show similar rates of photosynthesis at low light intensities, but high-light-acclimated cells appear to outperform the low-light-acclimated cells at high light intensities. When the rates of photosynthesis are normalized to cell number (Fig. 3.7b), it is clear that low-light-acclimated cells have higher rates of photosynthesis at low light intensities, while high-light-acclimated cells have higher rates of photosynthesis at high light intensities. Finally, when photosynthesis is normalized to cell carbon (Fig. 3.6c), the low-light-acclimated cells have higher rates of photosynthesis than high-light-acclimated cells at all light intensities. This last approach has the advantage of showing the effect of variations in the *P* vs. *E* curve on the rate of incorporation of carbon into cell biomass under some conditions.

Physiological acclimation to variations in irradiance serves to minimize variations in growth rate when light varies. For phytoplankton, this entails a balance between the light and light-independent reactions of photosynthesis. At low irradiance, photosynthesis is limited by the rate of light absorption and photochemical energy conversion. At

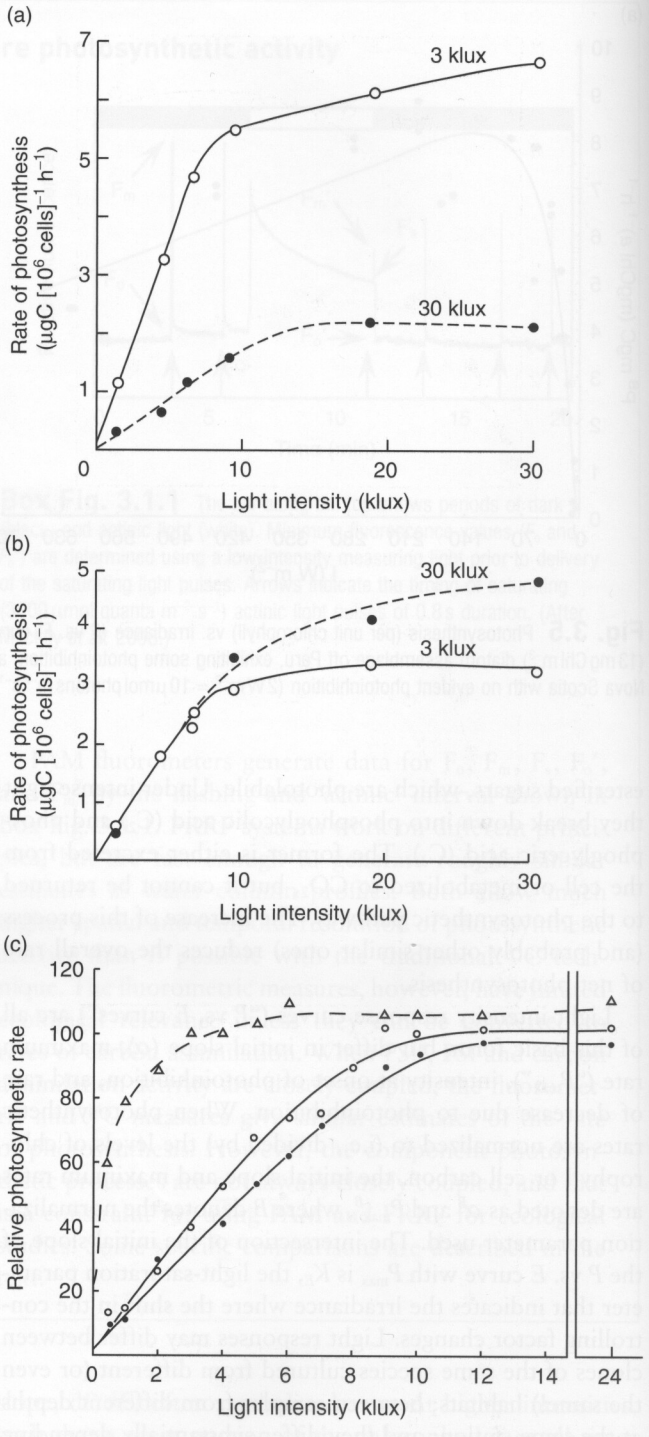

Fig. 3.6 Three types of acclimation to different light intensities, all in terms of photosynthesis per cell, not per unit chlorophyll. Changing chlorophyll per cell is part of the acclimation process. (a) *Chlamydomonas moevuss*. (b) *Cyclotella meneghiniana*. (c) *Phaeodactylum tricornutum*. Light intensities were 12 (dots), 5 (circles) and 0.7 (triangles) klux. (a after Jørgensen 1969, b after Jørgensen 1964, c after Beardall & Morris 1976.)

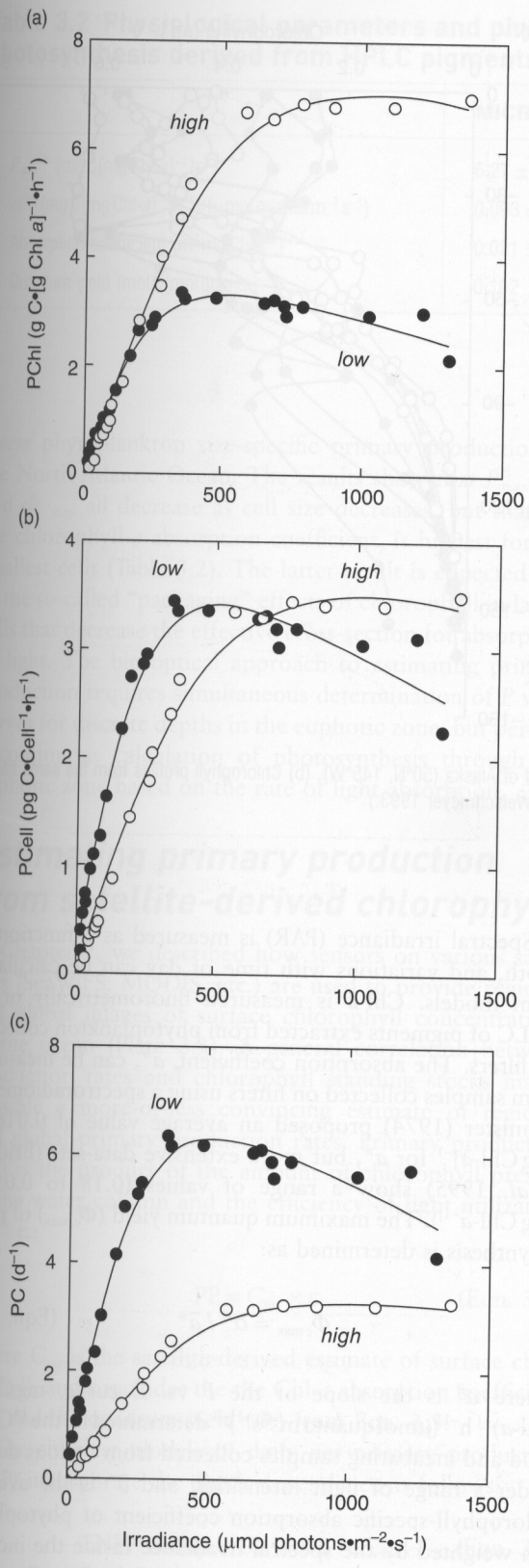

Fig. 3.7 *P* vs. *E* response curves for high-light (1200 μmol photons m^{-2} s^{-1}) and low-light (50 μmol photons m^{-2} s^{-1}) acclimated nutrient-replete cultures of the diatom *Skeletonema costatum*. (a) Chl-*a*-specific photosynthesis. (b) Cell-specific photosynthesis. (c) Carbon-specific photosynthesis. (After MacIntyre *et al.* 2002.)

high irradiance, photosynthesis is limited by the rate of electron transport, level of RuBisCO, or supply of ribulose 1,5 bisphosphate for the fixation of carbon.

Models for photosynthesis

The basic *P* vs. *E* curve suggests directly how photosynthetic rates per unit biomass of phytoplankton should vary downward in the sea. In the layers closest to the surface, productivity will either be at P_{max} or photoinhibited. As measures are made deeper in the water column, they can be expected to increase to P_{max} as irradiance decreases below photoinhibiting levels, then remain at P_{max} for some distance downward as light absorption by water and particles (including phytoplankton) progressively reduces available irradiance. From some depth not very far down, irradiance will be in the sloped part of the *P* vs. *E* curve, so that photosynthetic output gets progressively less. Since irradiance declines exponentially with depth (according to Beer's Law, $E_z = E_0 e^{-kz}$, where k is the extinction coefficient and z is depth), the *P* vs. z relation decreases exponentially downward from the depth where irradiance is less than that forcing photoinhibition, as shown by vertical profiles (Fig. 3.8a) of ^{14}C-uptake data. Of course, the primary production per unit volume is also a function of the amount of phytoplankton present, usually characterized by the chlorophyll profile. In temperate and high latitudes (Fig. 3.8b), that is maximal and fairly even through the upper mixing layers, then tapers off.

Extinction of light with depth means that at some depth, fairly close to the surface, irradiance will be the primary factor limiting productivity. That is true everywhere in the oceans. When it is said that phytoplankton growth is nutrient-limited, reference is to the upper water column or *euphotic* zone. The photosynthetic compensation depth varies with surface irradiance and the absorption coefficient (k), and is often assumed to be the depth at which irradiance is 1% of the surface value, maximally 70 m at lowest k(–0.067). However, subtropical gyres with minimal k have a strongly shade-adapted flora in the deeper euphotic zone forming a "deep chlorophyll maximum" (Fig. 3.9) around 100 m (~0.1% of the surface irradiance) in which net photosynthesis is still positive. This very widespread feature of the subtropical and tropical oceans is due to large amounts of chlorophyll per cell resulting from shade acclimation, although changes in species composition also contribute to some of the differences.

Bio-optical models of primary production

Bio-optical models of primary production (*P*) take the general form of:

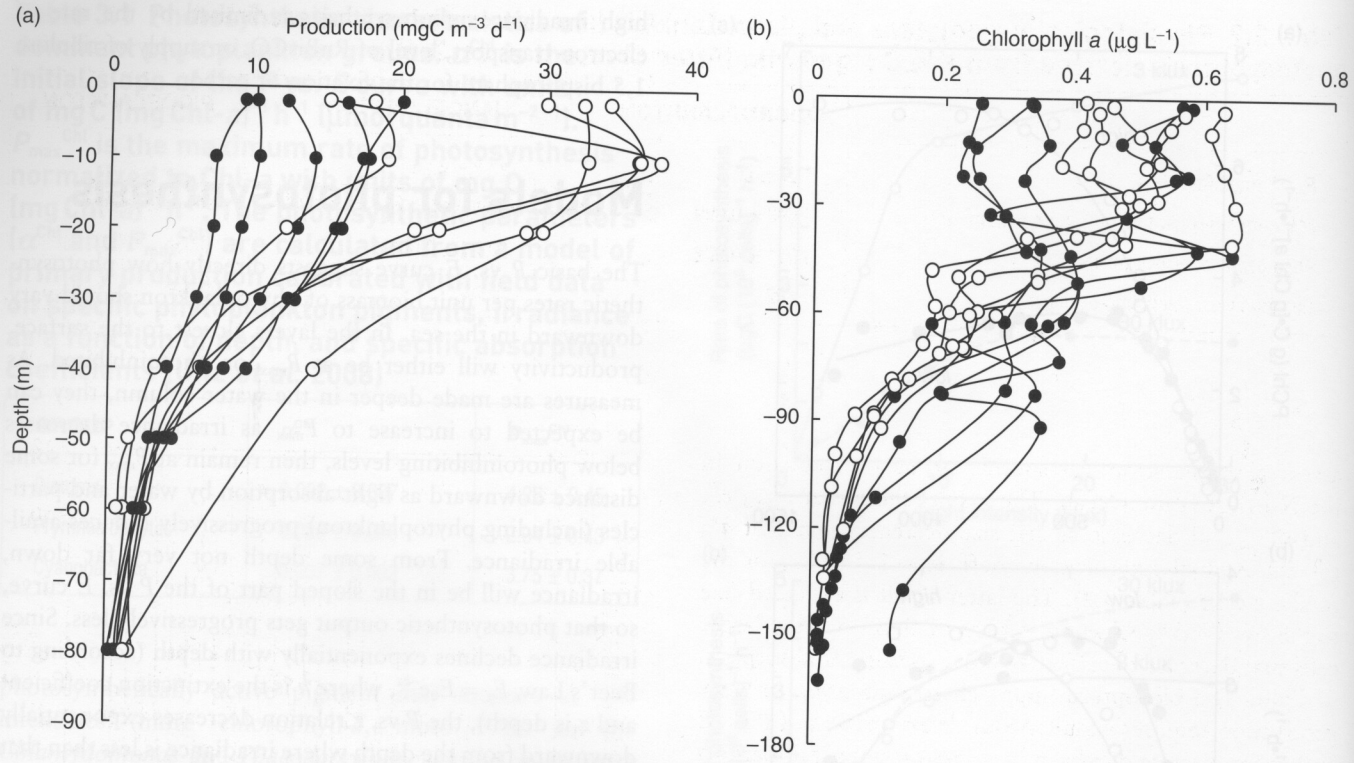

Fig. 3.8 (a) May (•) and September (○) profiles of primary productivity m^{-3} in the Gulf of Alaska (50°N, 145°W). (b) Chlorophyll profiles from the same site at various times are always maximal near the surface, and then taper off below 50 m. (After Welschmeyer 1993.)

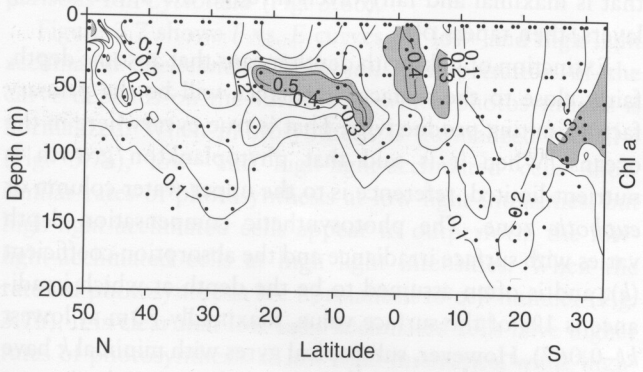

Fig. 3.9 A vertical chlorophyll section from 49°N to 33°S in the Atlantic Ocean. North of 45°N and south of 40° the chlorophyll maximum is in the upper 50 m. Deep chlorophyll maxima occur in the subtropical gyres between 100 and 175 m depth. Surface outcropping and a shallow (50 m) subsurface maximum occur within the equatorial band. (After Serret *et al.* 2006.)

$$P = \mathrm{PAR} \times [\text{Chl-}a] \times a^* \times \Phi_c \qquad \text{(Eqn. 3.2)}$$

where PAR (mol quanta m^{-2} s^{-1}) is the photosynthetically available radiation, [Chl-*a*] is the chlorophyll-*a* concentration (mg m^{-3}), a^* is the Chl-*a* absorption coefficient (m^2 [mg Chl-a^{-1}]), and Φ_c is the quantum efficiency for carbon fixation (mol C[mol quanta]$^{-1}$).

Spectral irradiance (PAR) is measured as a function of depth, and variations with time of day can be calculated from models. Chl-*a* is measured fluorometrically or by HPLC of pigments extracted from phytoplankton collected on filters. The absorption coefficient, a^*, can be measured from samples collected on filters using a spectroradiometer. Bannister (1974) proposed an average value of 0.016 m^2 [mg Chl-a]$^{-1}$ for a^*, but more extensive data-sets (Bricaud *et al.* 1995) show a range of values (0.18 to 0.01 m^2 [mg Chl-a^{-1}]). The maximum quantum yield ($\Phi_{c\,max}$) of photosynthesis is determined as:

$$\Phi_{c\,max} = \alpha^B / \overline{a}^* \qquad \text{(Eqn. 3.3)}$$

where α^B is the slope of the P vs. E curve, mg C (mg Chl-a)$^{-1}$ h^{-1} (μmol quanta m^{-2} s^{-1})$^{-1}$ determined by the ^{14}C method and incubating samples collected from various depths under a range of light intensities, and $\overline{a}^*$ is the average chlorophyll-specific absorption coefficient of phytoplankton weighted by the spectral irradiance inside the incubation chambers used for determination of the P vs. E curves.

Claustre *et al.* (2005) used this particular bio-optical model combined with quantitative information on the composition of the phytoplankton community derived from HPLC pigment concentrations (Bricaud *et al.* 2004) to

Table 3.2 Physiological parameters and phytoplankton biomass variables for modeled photosynthesis derived from HPLC pigments. (After Claustre *et al.* 2005.)

	MICROPLANKTON	NANOPLANKTON	PICOPLANKTON
P_{max}^{Chl} (mg C[mg Chl-*a*]$^{-1}$ h^{-1})	6.27 ± 0.53	2.38 ± 0.23	0.13 ± 0.3
α^{Chl} (mg C[mg Chl-*a*]$^{-1}$ h^{-1})/(μmol quanta m^{-2} s^{-1})	0.093 ± 0.009	0.046 ± 0.004	0.014 ± 0.005
Absorption coefficient (m^2 mg Chl a^{-1})	0.021 ± 0.002	0.021 ± 0.001	0.038 ± 0.001
Quantum yield (mol C[mol quanta]$^{-1}$)	0.102	0.050	0.009

assess phytoplankton size-specific primary production in the North Atlantic Ocean. The results show that P^B_{max}, α^B, and $\Phi_{c\ max}$ all decrease as cell size decreases, but that a^*, the chlorophyll-*a* absorption coefficient, is highest for the smallest cells (Table 3.2). The latter result is expected due to the so-called "packaging" effects of chlorophyll in larger cells that decrease the effective cross-section for absorption of light. The bio-optical approach to estimating primary production requires simultaneous determination of *P* vs. *E* curves for discrete depths in the euphotic zone, but permits a continuous calculation of photosynthesis through the euphotic zone based on the rate of light absorption.

Estimating primary production from satellite-derived chlorophyll

In Chapter 2, we described how sensors on various satellites (SeaWiFS, MODIS, etc.) are used to provide regional and global images of surface chlorophyll concentrations in the ocean (Plate 2.3). A general correlation between production rates and chlorophyll standing stocks makes possible a more-or-less convincing estimate of regional and global primary production rates. Primary production (PP) is the product of the amount of chlorophyll present in the water column and the efficiency of light utilization (ε), i.e.:

$$PP = C_{sat} \times \varepsilon \qquad \text{(Eqn. 3.4)}$$

where C_{sat} is the satellite-derived estimate of surface chlorophyll, and ε includes the the Chl-*a* absorption coefficient (a^*) and the quantum yield (Φ_c) from Eqn. 3.3.

The simplest models of daily net primary production (NPP) incorporate the depth dependence as follows:

$$\Sigma NPP = P^b_{opt} \times C_{sat} \times DL \times Z_{eu} \times F \qquad \text{(Eqn. 3.5)}$$

where P^b_{opt} is the maximum value of Chl-normalized photosynthesis in the water column (similar to P^b_{max}); *DL* is the duration of the photoperiod; Z_{eu} is the depth of the euphotic zone (depth of 1% surface PAR); and *F* describes the

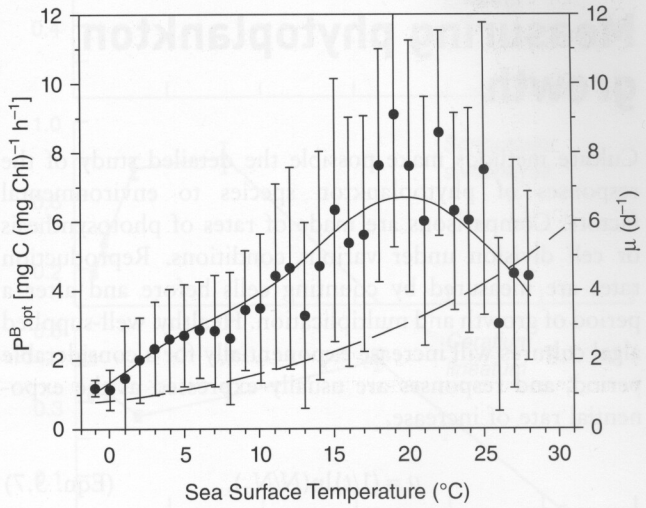

Fig. 3.10 Measured (•; ± SD) and modeled median value (solid curve) of the photoadaptive parameter, P^B_{opt}, as a function of sea-surface temperature. Dashed curve indicates the theoretical maximum specific growth rate (μ; d^{-1}) of phytoplankton described by Eppley (1972), which is used in a variety of productivity models. (After Behrenfeld & Falkowski 1997a.)

dependence of vertically integrated net primary production (ΣNPP) on the surface light intensity as it affects the depth of light-saturated photosynthesis.

Behrenfeld and Falkowski (1997a) compared measurements of P^b_{opt} with temperature (Fig. 3.10) and derived a single-factor empirical model for estimating the maximum value of Chl-normalized photosynthesis in the water column:

$$P^B_{opt} = -3.27\times10^{-8}T^7 + 3.4132\times10^{-6}T^6 - 1.348\times10^{4}T^5 + 2.462\times10^{-3}T^4 - 0.0205T^3 + 0.0617T^2 + 0.2749T + 1.2956. \qquad \text{(Eqn. 3.6)}$$

The error bars based on measured values of P^b_{opt} are wide and certainly contribute to the uncertainty in the

derived estimates of primary production, but the approximation appears to be adequate to represent regional differences in maps of global ocean productivity. Behrenfeld and Falkowski (1997b) also compared more elaborate time-integrated, wavelength-integrated and wavelength-resolved models for estimating primary production on global scales. The major difference among model outputs derives from the mode of estimation of P^{b}_{opt}, the "photoadaptive" variable. When the same chlorophyll fields are used in the models, global annual primary production in the ocean is about 44 Gt C yr^{-1}.

Measuring phytoplankton growth

Culture methods make possible the detailed study of the responses of phytoplankton species to environmental factors. Comparisons are made of rates of photosynthesis or cell division under various conditions. Reproduction rates are measured by counting cells before and after a period of growth and multiplication. Healthy, well-supplied algal cultures will increase exponentially for a considerable period, and responses are usually expressed as the exponential rate of increase,

$$\mu = (1/t)\ln(N/N_o), \qquad \text{(Eqn. 3.7)}$$

usually with units of d^{-1}, or as the number of cell divisions (doublings) per day,

$$\mu_2 = (1/t)\log_2(N/N_o). \qquad \text{(Eqn. 3.8)}$$

It is useful to memorize that if $\mu_2 = 1$, then $\mu = 0.69$.

If cells are growing under constant conditions, then the daily increase of any cellular component (e.g. carbon or nitrogen) can be measured and used to calculate a growth rate. Such conditions can be achieved in steady-state continuous cultures, but are not common for incubation times less than the generation period (doubling time) for phytoplankton. Growth rates can be determined as a function of nutrient concentration, using the Monod relationship (which is analogous to the more familiar Michaelis–Menten enzyme kinetic equation, see Chapter 1, pp. xx and Box 3.2):

$$\mu = \mu_{max}[S]/(K_s + [S]). \qquad \text{(Eqn. 3.9)}$$

Chan's (1978) data (Fig. 3.11) show that fully photoacclimated dinoflagellates typically reach maximal doubling rates at lower irradiance than diatoms, while diatoms have higher maximum growth rates. Actually, dinoflagellates and diatoms have the same photosynthetic rates per unit chlorophyll, but autotrophic dinoflagellates have much less chlorophyll relative to other cell constituents. When adapted to high irradiance, >200 µmol photons m^{-2} s^{-1}, typical dinoflagellates have 4 to 10 ng Chl (µg protein)$^{-1}$, whereas diatoms have 15 to 30 ng Chl (µg protein)$^{-1}$. Dinoflagellates also have a much more DNA than other algae, and consequently require more energy for cellular maintenance, giving them a lower growth efficiency (Tang 1996).

Illumination in the upper ocean is not continuous, but has a diel cycle (this is not news). It increases rapidly as the sun rises, peaks at noon, and drops to very low levels at night. Virtually all organisms, marine and terrestrial, have physiological cycles matched to the illumination cycle, and most have internal time-keeping processes allowing anticipation of events in the daily round. Algal growth and often multiplication vary with a daily periodicity, since photosynthesis must vary with the alternation of light and dark. Nelson and Brand (1979) have examined the phase relationships between cell division and the light–dark cycle for a variety of planktonic algae in culture. Timing of cell division tends to follow taxonomic lines (Fig. 3.12a & b).

Six species of diatom strongly favored daytime division. One species of dinoflagellate and six varied species of microflagellates had division maxima at night (Fig. 3.12c & d). There are counter-examples in the literature of dark-period division in diatoms (Eppley *et al.* 1971), but, on the whole, diatoms are diurnal dividers, while other forms divide at night. There are cycles in many other physiological parameters which parallel those of division.

Effects of nutrient availability

The organic matter of a typical phytoplankton assemblage in the sea has the following elemental composition in terms of atoms (or moles) relative to phosphorus:

$$C : N : P = 108 : 15.5 : 1$$

These numbers are known as the *Redfield ratios* after A.C. Redfield, who first measured them carefully in 1934 (see Redfield *et al.* 1963). Oxygen and hydrogen are also present in organic material, but clearly are never limiting in the marine environment. Carbon as carbonate (about 2 mM) is not limiting, either, although changes in abundance of the components of the carbonate system in seawater can alter the rate of photosynthesis. The quantities of fixed nitrogen and phosphorus in the ocean at great depth are in the rough ratio 16 : 1. The reason is that those elements are supplied to the deep sea primarily by decay of organic matter descending from above. Phosphorus and nitrogen are required for production of organic matter in roughly the Redfield ratios, and since

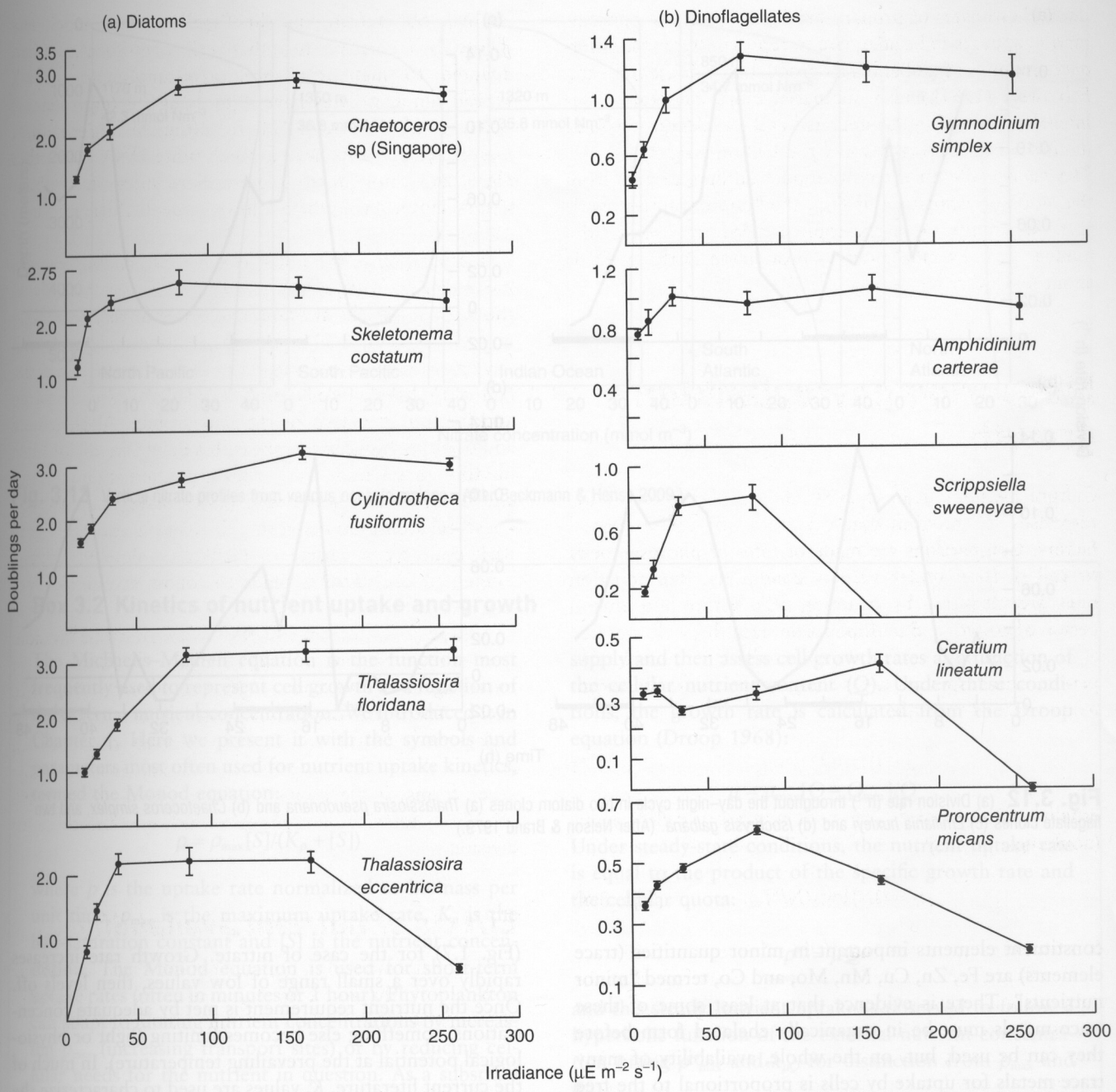

Fig. 3.11 Response of growth rates to changes in irradiance compared for diatoms (left) and dinoflagellates (right). These are exponential rates established after long acclimation at each irradiance. Bars are 95% confidence limits. (After Chan 1978.)

they are often in limited supply (rate of supply < (rate of demand for maximum growth rates), they partly control rates of phytoplankton production in the sea. They are known as "major nutrients". Silicon is also a major nutrient for diatoms and silicoflagellates. Each of these major nutrients shows characteristic vertical distributions in oceanic waters (Fig. 3.13) with low to non-detectable concentrations in the surface water, and increasing concentrations with depth, but with some differences in the location of the nutriclines (steepest gradients in concentration) depending on the depth and rates of remineralization processes.

In addition, all phytoplankton have small, but important, requirements for a wide array of other elements. Particularly important are transition metals and common ions. Growth of phytoplankton could be limited by the supply of any of these. However, many (Na^+, Cl^-, SO_4^{2-}, Mg^{2+}, Ca^{2+}) are present far in excess of need. Thus,

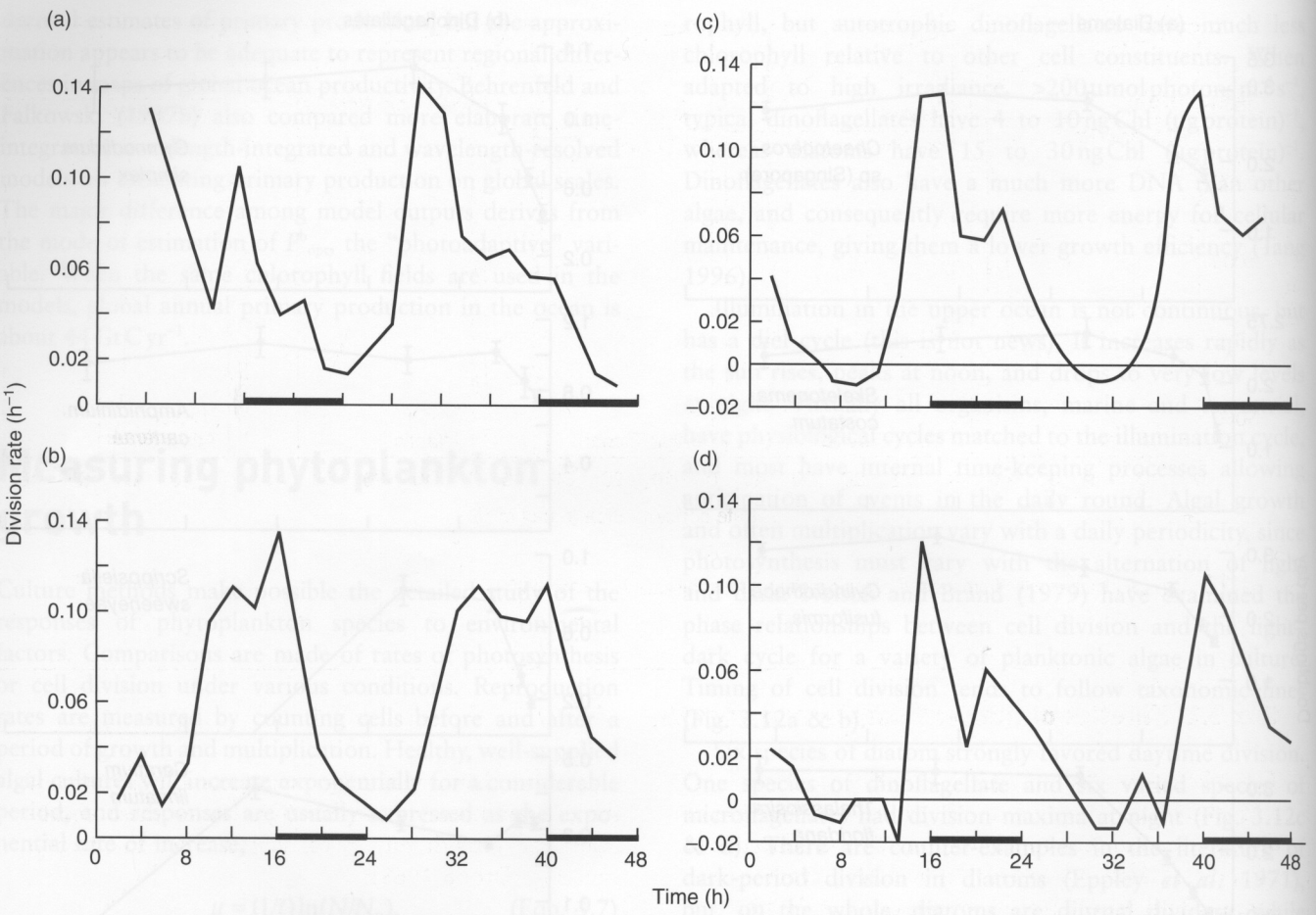

Fig. 3.12 (a) Division rate (h^{-1}) throughout the day–night cycle in two diatom clones (a) *Thalassiosira pseudonana* and (b) *Chaetoceros simplex*, and two flagellate clones (c) *Emiliania huxleyi* and (d) *Isochrysis galbana*. (After Nelson & Brand 1979.)

constituent elements important in minor quantities (trace elements) are Fe, Zn, Cu, Mn, Mo, and Co, termed "minor nutrients". There is evidence that at least some of these trace metals must be in organically chelated form before they can be used, but, on the whole, availability of many trace metals for uptake by cells is proportional to the free ion activity. Interference of trace metals with one another (some can occupy and block the uptake sites for the others) is another important aspect of phytoplankton nutrition. Finally, some of the vitamins needed for human nutrition are required as growth supplements by many species of phytoplankton. Such vitamins, particularly thiamin, biotin, and B_{12} (a protein-bound form of cobalamin), are present in small amounts in seawater, sometimes becoming reduced to limiting levels.

The kinetics of phytoplankton growth and uptake rates as a function of nutrient concentration are hyperbolic functions of various forms (Box 3.2). The response of phytoplankton growth to a range of concentrations of a single limiting nutrient (other nutrients in excess) is illustrated (Fig. 1.7) for the case of nitrate. Growth rate increases rapidly over a small range of low values, then levels off. Once the nutrient requirement is met by adequate concentrations, something else becomes limiting (light or physiological potential at the prevailing temperature). In much of the current literature, K_s values are used to characterize the phytoplankton growth responses to nutrient availability (Table 3.3). Small K_s values indicate rapid response of the growth rate to increased nutrient availability. Large K_s indicates that relatively high concentration is required to achieve a near-maximal growth rate.

Determination of the responses of phytoplankton species and phytoplankton assemblages to variation in nutrient availability took much of the effort in phytoplankton ecology from 1970 to 1990. The data are complex and various. Note that the results in Fig. 1.7 are presented as doublings/day, a specific growth rate (growth/abundance/time). That is the ideal form for information on nutrient responses. However, many of the data available are as nutrient uptake rates combined with one determination of

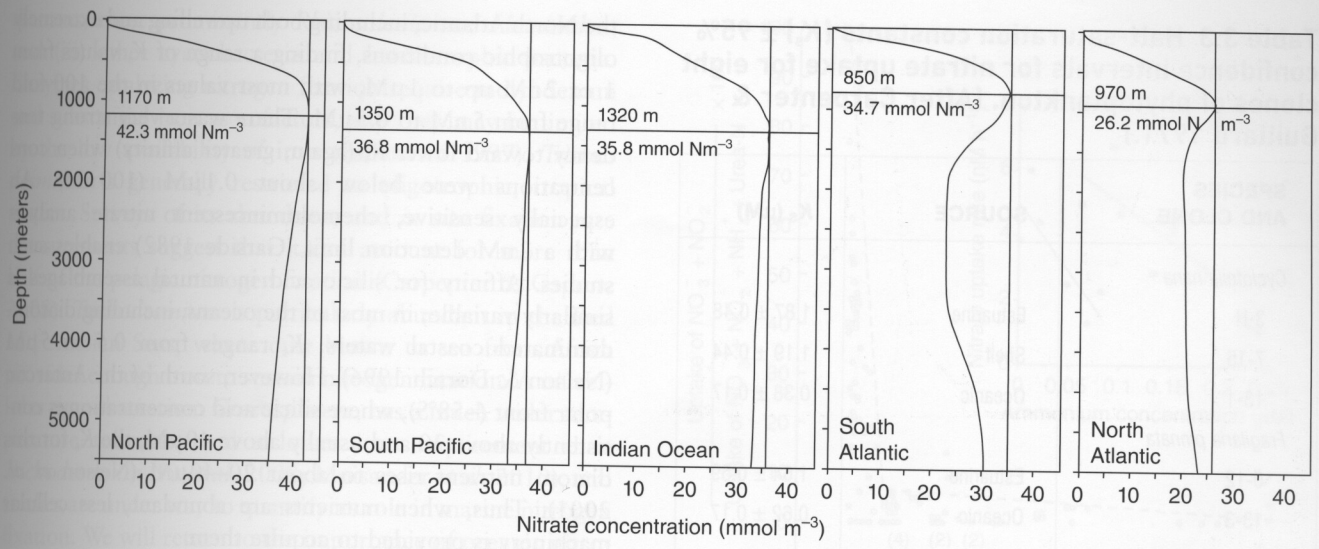

Fig. 3.13 Vertical nitrate profiles from various oceanic regions. (After Beckmann & Hense 2009.)

Box 3.2 Kinetics of nutrient uptake and growth

The Michaelis–Menten equation is the function most frequently used to represent cell growth as a function of the external nutrient concentration. We introduced it in Chapter 1. Here we present it with the symbols and parameters most often used for nutrient uptake kinetics, termed the Monod equation:

$$\rho = \rho_{max}[S]/(K_\rho + [S])$$

where ρ is the uptake rate normalized to biomass per unit time, ρ_{max} is the maximum uptake rate, K_ρ is the half-saturation constant and $[S]$ is the nutrient concentration. The Monod equation is used for short-term uptake rates (often in minutes or 1 hour). Phytoplankton can adapt to limiting nutrient concentrations by increasing ρ_{max} (increasing transport sites) or by reducing cellular needs for the nutrient in question. As a substrate (e.g. nutrient) affinity measure, K_ρ must be used with care, because it is affected by ρ_{max}. If their ρ_{max} values are different, two hyperbolae with the same initial slope will have different K_ρ values. Larger ρ_{max} forces a larger K_ρ. Kristiansen *et al.* (2000) give a nice example of this effect.

For steady-state conditions, the Monod equation can be used to describe growth rate as a function of substrate concentration:

$$\mu = \mu_{max}[S]/(K_\mu + [S]).$$

Another approach to examining kinetics of nutrient uptake is to grow cultures with a continuous nutrient supply and then assess cell growth rates as a function of the cellular nutrient content (Q). Under these conditions, the growth rate is calculated from the Droop equation (Droop 1968):

$$\mu = \mu_{max}[Q - Q_{min}]/Q$$

Under steady-state conditions, the nutrient uptake rate is equal to the product of the specific growth rate and the cellular quota:

$$\rho^{ss} = \mu Q$$

and this steady nutrient uptake is observed to follow a hyperbolic function of the external nutrient concentration (using $\rho^{ss}{}_{max}$ and $k_{\mu Q}$ for distinction from ρ_{max} and k_ρ:

$$\rho^{ss} = \rho^{ss}{}_{max}[S]/(K_{\mu Q} + [S])$$

Morel (1987) describes the derivations and applications in more detail.

Both the Monod and Droop equations have been useful for the study of nutrient uptake and growth kinetics for cultured phytoplankton under steady-state conditions. The Monod model is simpler and preferred for steady-state conditions, while the Droop model is more complex and has the additional requirement of determining the variations in cell quota but it performs better under transient conditions.

Table 3.3 Half-saturation constants (K_s) ± 95% confidence intervals for nitrate uptake for eight clones of phytoplankton. (After Carpenter & Guillard 1971.)

SPECIES AND CLONE	SOURCE	K_s (μM)
Cyclotella nana		
3-H	Estuarine	1.87 ± 0.48
7-15	Shelf	1.19 ± 0.44
13-1	Oceanic	0.38 ± 0.17
Fragilaria pinnata		
0-12	Estuarine	1.64 ± 0.59
13-3	Oceanic	0.62 ± 0.17
Bellerochia sp.		
Say-7	Estuarine	6.87 ± 1.38
675D	Shelf	0.12 ± 0.08
SD	Oceanic	0.25 ± 0.18

the maximum growth rate at high nutrient concentration to produce a synthetic μ vs. [S] curve.

Equality of the uptake and growth curves is ensured (forced) in many studies by use of *chemostats* for determination of uptake rates. A chemostat is a container of well-mixed nutrient medium to which new nutrient solution is supplied at a volume rate (e.g. ml min^{-1}) μ_1, and from which culture is removed at a volume rate μ_2. The volume is maintained constant by choosing $\mu_1 = \mu_2$. Measurements of phytoplankton growth rate are made at system equilibrium by counting the number of cells per unit volume in the outflow and dividing by [flow rate/chamber volume]. Nutrient uptake rate per cell is equal to the difference in concentration between inflow and outflow divided by the flow rate and cell count in the chamber at steady-state. *Turbidostats*, used for example by Falkowski *et al.* (1985), have several advantages over chemostats. Turbidostat inflow and outflow are controlled by feedback from a particle-density sensor, allowing the stock to rise to equilibrium level without having to "fight" the outflow during "spin-up". Another (not used by Falkowski *et al.* 1985) is that the turbidostat can incorporate natural light cycling by reducing the outflow when growth or multiplication rates drop or rise. Rates then must be averaged over the diel cycle to compare effects of nutrient levels.

Affinity for nutrients in natural phytoplankton assemblages is extremely variable, but greater uptake capability (represented by lower K_s values) is generally observed as nutrient concentration goes down. Harrison *et al.* (1996) studied nitrate uptake kinetics from about 10°N to 63°N in the North Atlantic, including both upwelling and extremely oligotrophic conditions, finding a range of K_s values from 1 or 2 nM up to 1 μM, with most values in the 100-fold range from 5 nM to 0.5 μM. There was a very strong tendency toward lower K_s (again, greater affinity) when concentrations were below about 0.1 μM (100 nM). An especially sensitive, chemolumincescent nitrate analysis with a 2 nM detection limit (Garside 1982) enables such studies. Affinity for silicic acid in natural assemblages is similarly variable; in most of the oceans, including diatom-dominated coastal waters; K_s ranges from 0.5 to 5 μM (Nelson & Dortch 1996). However, south of the Antarctic polar front (~58°S), where silicic acid concentration is consistently above 20 and usually above 40 μM, the K_s for this diatom nutrient rises to about 20–40 μM (Nelson *et al.* 2001). Thus, when nutrients are abundant, less cellular machinery is provided to acquire them.

Nitrogen

Nitrogen is in a sense the most informative phytoplankton nutrient. That is because its oxidation states give information about the biological transformations to which given atoms have been subjected in the immediate past. Because of this information content, early studies of nutrient-uptake kinetics and regulation of phytoplankton growth focused on nitrate and ammonium utilization. Physiological and ecological studies have since broadened to include trace metals, co-limiting factors, and organic forms of nitrogen and phosphorus. Nitrogen is a fundamental constituent of proteins, nucleic acids, enzyme cofactors and at least one key, marine carbohydrate, chitin. Thus, it must be acquired and incorporated by phytoplankton for the initial synthesis of organic matter, and it remains essential at all steps in all food chains. However, very few organisms are capable of directly reducing and incorporating N_2, the form of nitrogen in the atmosphere that is abundant as dissolved gas in the ocean. This capability is restricted to an array of bacteria, some of which are photosynthetic cyanobacteria ("blue-green algae"). The biochemical transformations are referred to as "nitrogen fixation." They require a high energy input for reduction of N_2 to ammonium, which then can be incorporated in amino acids, purines, glucosamine, and so forth. Ammonium in marine systems can serve as an energy source for bacteria and archaea, which oxidize it to nitrite (NO_2^-), then nitrate (NO_3^-). Both NO_2^- and NO_3^- are available for uptake by most phytoplankton and many bacteria. Because they are biologically available, all these reduced and oxidized forms are referred to as "fixed" nitrogen.

Pelagic marine nitrogen fixation is estimated to be 121×10^9 kg N yr^{-1} (Galloway *et al.* 2004). Fixation is mediated by (i) the filamentous cyanophyte *Trichodesmium*; (ii) *Richelia*, a bacterium living endosymbiotically in several

diatoms, most prominently *Rhizosolenia* and *Hemiaulus*; and (iii) other cyanobacteria and heterotrophic bacteria. Enzymes catalyzing nitrogen fixation require molybdenum and substantial iron as cofactors, and they may be limited by the low availability of iron (Falkowski 1997). *Trichodesmium* is generally restricted to oligotrophic, tropical waters. Surveys of its abundance and *in situ* fixation rate measurements suggest that it can account for more than half of the pelagic nitrogen fixation (Carpenter & Capone 2008). *Trichodesmium* is particularly abundant in the Red and Arabian Seas, where dust blown to sea from Africa provides enough iron to sustain nitrogen fixation. A unicellular cyanobacterium *Crocosphaera*, has a much wider temperature tolerance and a lower iron requirement than *Trichodesmium* (Fu *et al.* 2008; Moisander *et al.* 2010), and studies are under way to quantify its role in marine nitrogen fixation. We will return to the importance of oceanic nitrogen fixation in Chapter 11.

A key fact about the pelagic nitrogen cycle is that its redox transformations are vertically separated. When proteins or nucleic acids are metabolized, say by heterotrophs, the most usual form for excretion of free nitrogen is ammonium, but a fraction is in urea or uric acid – small organic molecules less toxic than ammonium in internal solution. Nitrogen in these forms is reduced. Eukaryotic heterotrophs do not use these reduced forms as fuel. Moreover, archaeal oxidation of ammonium to nitrite and bacterial oxidation of nitrite to nitrate appear to be inhibited by light, so both processes mostly occur below the euphotic zone. Because of the inhibition, "nitrifying" bacteria cannot build up a stock to take advantage of ammonium even at night. Finally, in euphotic zones, phytoplankton take up ammonium and urea in preference to oxidized forms of fixed nitrogen (Fig. 3.14). So, their concentrations are held at low levels, rarely exceeding 0.5 μM, except in estuaries.

Fixed nitrogen, like all nutrients, is eroded from the euphotic zone by the downward movement of photosynthetically generated organic matter. This occurs through the sinking of phytoplankton; vertical mixing of particles and dissolved organic matter; sinking of particulate wastes of grazers; and downward swimming of zooplankton and fish. Subsequent mineralization of organic matter introduces ammonium at depth, where nitrifiers can function. The second oxidation step, mediated by *Nitrobacter*, is more light-inhibited than the first, which is mediated in the ocean by archaea, so there is generally a thin layer with measurable concentration of NO_2^-. Below that, most fixed nitrogen is oxidized to NO_3^-. In most regions, the most important return supply of fixed nitrogen to the upper layer is the upward return of nitrate by vertical mixing, which is often seasonally accentuated, and by upwelling, which is geographically localized. Once in the euphotic zone, nitrate can be returned to the biological cycle through uptake by phytoplankton.

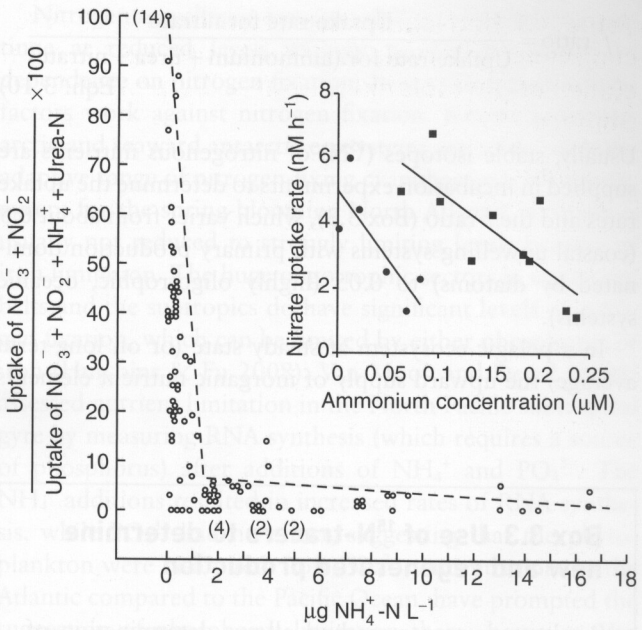

Fig. 3.14 Ratio of nitrate uptake to total fixed nitrogen uptake (the *f*-ratio) versus available ammonium concentration in Chesapeake Bay (from McCarthy *et al.* 1975). Inset: nitrate uptake rate vs. available ammonium estimated with $^{15}NO_3^-$ in the oceanic subarctic Pacific. (After Wheeler & Kokkinakis 1990.) In both habitats, ammonium availability suppresses nitrate utilization by phytoplankton.

Because production based on nitrate is using nutrient molecules newly arrived from outside the productive layer, it is termed *new production*. If the organic matter is then eaten, respired, and the nitrogen excreted as ammonium, its subsequent uptake and reincorporation in organic matter by phytoplankton is termed *recycled production*. This key distinction was spelled out by Dugdale & Goering (1967) in a seminal paper. At the time the paper was written, it was assumed that, by and large, fixed nitrogen was the usual limiting nutrient, so that ultimately the rates of the system would be set by the rate of supply of nitrate. Later it has become clear that availability of other nutrients, particularly iron, can set the rate of nitrate utilization. Iron is required for some components of the photosynthetic electron-transport systems and for nitrate reductase, an enzyme functioning to reduce nitrate to ammonium. Nonetheless, the rate of nitrate utilization remains a good measure of the new production. The rate of ammonium utilization is, in the same sense, a measure of recycled production. In ecosystems with very low nitrate, or high nitrate but low iron, the recycled production can be a much larger fraction of carbon fixation than new production. In systems with both nitrate and iron, new and recycled production are more equal. The relative importance is expressed as the "*f*-ratio":

$$f\text{-ratio} = \frac{\text{Uptake rate for nitrate}}{\text{Uptake rate for (ammonium + urea + nitrate)}} \quad \text{(Eqn. 3.10)}$$

Usually, stable isotopes (^{15}N) of nitrogenous nutrients are supplied in incubation experiments to determine the uptake rates and the *f*-ratio (Box 3.3), which varies from about 0.5 (coastal upwelling systems with primary production dominated by diatoms) to 0.05 (highly oligotrophic, oceanic systems).

In a pelagic ecosystem at steady state (or on long-term average) the upward supply of inorganic nutrient elements by vertical mixing and advection into the euphotic zone should be equal to the downward flux at the base of the euphotic zone of those same elements incorporated in organic matter. Downward flux includes sinking of organic particles and vertical mixing in downward-decreasing gradients of dissolved and particulate organic matter. Thus, another way to estimate new production is to catch falling organic particles in traps moored at an appropriate depth in the water column and then determine the amount of carbon in the flux. Rates per unit area are determined by dividing the organic content after a trapping interval by trap area and time of deployment. Elskens *et al.* (2008) used tracer experiments and neutrally buoyant sediment traps to measure and compare new production and export production in the mesotrophic subarctic Pacific (47°N, 161°E). New production in the upper 50 m was about 20% of total primary production, while export production measured in traps at 150 m was about 10% of total primary production. Elskens *et al.* also estimated rates of remineralization and found that 80% of remineralization was in the upper 50 m, and 11% in the 50–150 m portion of the water column. Satellite measures of surface chlorophyll and deeper trap studies indicated that the Elskens *et al.* traps were deployed at the end of a diatom bloom. There was little change in phytoplankton biomass in the upper 150 m. The carbon and nitrogen assimilated during primary production were mostly consumed and remineralized by heterotrophs in the upper 150 m, and about 9% of the primary production sank into deeper water.

Elemental cycles are generally not in continuous balance. During seasons of more rapid primary production, dissolved, colloidal and particulate organic matter accumulates in the euphotic zone (Wheeler 1993). Recycling of this molecular detritus can require all the rest of the annual cycle. Thus, short-term trapping results will generally be less (apart from sampling problems) than short-term new production estimates.

New production should also be equivalent to the net oxygen production, [photosynthesis – respiration, PS – *R*] in the euphotic zone, since regenerated production is coupled to community respiration of photosynthate. There are severe difficulties in determining this in the field, particularly a requirement for precise estimation of oxygen-exchange rates at the sea surface. The concentrations of inert gases must also be measured to separate the effects of physical versus biological processes leading to supersaturation of gases in the surface mixed layer. Emerson *et al.* (1991) used argon and N_2 to estimate the effects of temperature and bubble processes on gas exchange rates between surface seawater and the atmosphere in the subarctic Pacific during the summer. The difference in saturation state between argon and oxygen indicates the biological component of O_2 supersaturation. Net oxygen production rates agreed reasonably well with ^{15}N estimates of new production for the summer samplings. To determine sea-

Box 3.3 Use of ^{15}N-tracers to determine new and regenerated production

An isotopic tracer method allows determination of these rates. It is based on labeling the fixed nitrogen supply, in bottle incubations of natural phytoplankton (much like a ^{14}C-uptake experiment) with nitrogen-15. After an interval of incubation, the ^{15}N incorporated from nitrate, or from a reduced form, into organic matter is determined by filtering the incubated water, and by recovering incorporated ^{15}N by destructive oxidation of the organic matter. The nitrogen is converted to N_2, then the $^{15}N/^{14}N$ ratios are determined by mass spectrometry or from emission spectra of the gas when excited by a high-voltage electric field. Each form of fixed nitrogen to be tested requires a separate labeling experiment. This technique is not perfect. Particularly, it is difficult to add sufficient $^{15}NH_4^+$ (or labeled urea) to get a signal, that is a shift in the $^{15}N/^{14}N$ ratio of phytoplankton, without significantly increasing total NH_4^+. That quickly enhances NH_4^+ usage and reduces NO_3^- uptake. In waters with very low nitrate, tracer additions of $^{15}NO_3$ can increase productivity overall. Another problem (e.g. Bronk & Glibert 1994) is that recovering and accounting for all added tracer is difficult, because some incorporated nitrogen ends up as dissolved organic matter outside cells. Nevertheless, ^{15}N methods have shown the broad outlines of the pelagic nitrogen cycle. Roughly, new production is proportional to the $^{15}NO_3^-$ uptake rate, and regenerated production is proportional to the $^{15}NH_4^+$-uptake rate. Because the ^{14}C method is believed to estimate the total of new and regenerated production, the ratio of [New/(New + Regenerated)], measured by isotope uptake rates, is multiplied by the ^{14}C-uptake rate to determine the new production in terms of carbon.

sonal and annual estimates of net oxygen production, Emerson *et al.* have used *in situ* measurements of O_2 and N_2 in surface waters. Nitrogen gas can be used as an "inert" gas because rates of nitrogen fixation only change the concentration by ~0.1%. By measuring temperature, salinity, oxygen, and total dissolved gas pressure every two hours on a mooring at the Hawaii Ocean Time series, Emerson *et al.* (2008) determined a net biological oxygen production in the surface mixed layer of $4.8 \pm 2.7\,\text{mol}\,O_2\,m^{-2}\,yr^{-1}$. Emerson and Stump (2010) used the same method to measure net oxygen production in the subarctic Pacific. Measurements taken every three hours for nine months on a surface mooring indicated a mean summertime oxygen production of $24\,\text{mmol}\,O_2\,m^{-2}\,d^{-1}$, and very little net oxygen production during the winter. Net oxygen production can be scaled to carbon production using a photosynthetic quotient (mol O_2 evolved : mol CO_2 consumed) of 1.45. For both of these studies, net oxygen production rates agreed well with other estimates of new production, but lack of precision in the estimates of the physical processes results in an uncertainty of about 40% for the rates of net oxygen production.

Phosphate

Phosphorus, available in the ocean as phosphate (PO_4^{3-}), is incorporated in many biological molecules, for example, nucleic acids, and adenosine di- and triphosphates (ADP and ATP). Esterification of a phosphate group to a small molecule creates a diffusible, high-energy "currency" suitable for enzyme binding at sites adjacent to binding of substrates. Hydrolysis of the ester bond (dephosphorylation) then provides energy ($-62\,\text{kJ}\,\text{mol}^{-1}$) for substrate transformations. Phosphate in the ocean comes only from rocks, and it is ultimately removed from the ocean by incorporation in sediments. In the meantime, it cycles as a nutrient much as fixed nitrogen, but without an informative variety of oxidation states. In highly oligotrophic environments (central gyres), a significant fraction of dissolved phosphate is in small organophosphate compounds, and at least some phytoplankton in those regions bear surface enzymes which can remove phosphate from organophosphorus and incorporate it.

In general, and despite debates about the matter (Falkowski 1997; Cullen 1999; Tyrrell 1999), phosphate is the principal limiting nutrient for planktonic photosynthesis in freshwater systems but not in marine ones. That is because fresh water is always closely associated with land, and thus is better supplied with iron. Iron enables nitrogen fixation in cyanophytes, which can then carry on photosynthesis until phosphate is exhausted. In coastal marine systems, nitrate simply runs out first, which Tyrrell (1999) shows with a graph based on widely dispersed NO_3^- and PO_4^{3-} observations (Fig. 3.15). At low levels, phosphate is often positive when nitrate is at zero, usually not the opposite.

Nitrogen recycling is fast enough for production to continue at reduced levels without forcing the system to dependence on nitrogen fixation. In oceanic waters several factors work against nitrogen fixation. Subarctic, subantarctic and seaward antarctic ecosystems are colder than the adaptive range of nitrogen-fixing cyanobacteria. Moreover, except for the spring-blooming North Atlantic, nitrogen is usually not reduced to strongly limiting levels because of iron limitation. The huge oligotrophic sectors in equatorial belts and the subtropics do have significant levels of nitrogen fixation, which can be limited by either phosphorus or iron (Hutchins & Fu 2008). Van Mooy and Devol (2008) assessed nutrient limitation in the North Pacific subtropical gyre by measuring RNA synthesis (which requires a source of phosphorus) after additions of NH_4^+ and PO_4^{3-}. The NH_4^+ additions resulted in increased rates of RNA synthesis, while PO_4^{3-} had no effect, suggesting that the phytoplankton were N-limited. Low PO_4^{3-} concentrations in the Atlantic compared to the Pacific Ocean, have prompted the suggestion of phosphorus limitation there; however, Van Mooy *et al.* (2009) elucidated an intriguing adaptation of Atlantic phytoplankton to low phosphorus. Phytoplankton in the Sargasso Sea reduce their cellular phosphorus requirements by substituting non-phosphorus membrane lipids for phospholipids. The *Prochlorococcus* genome is radically minimized (Dufresne *et al.* 2003), further saving on phosphate.

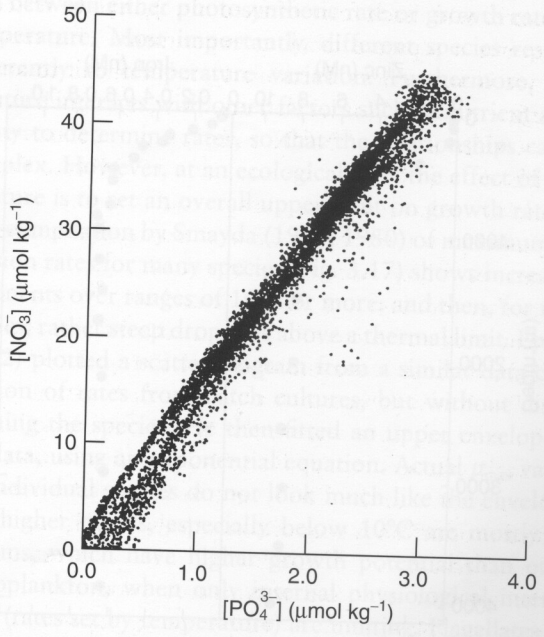

Fig. 3.15 A scatter plot from a series of global sampling sections (GEOSECS) of nitrate (NO_3^-) vs. phosphate (PO_4^{3-}). Some phosphate is usually left when nitrate is depleted below levels detected by standard techniques. (After Tyrrell 1999.)

Use of organic forms of nitrogen and phosphorus

Potential nutrients for phytoplankton growth (as well as heterotrophic organisms) include organic forms of nitrogen and phosphorus. These can be a significant component of the dissolved nutrient inventories in some regions, and net changes over annual cycles suggest that use of organic forms of nutrients may extend the productive season after inorganic forms are depleted (Banoub & Williams 1973). There are multiple sources and sinks for dissolved organic material, so generalizations about their significance are difficult, except to say that: (i) pool sizes are small; (ii) turnover rates can be high; and (iii) it can be difficult to separate the roles of autotrophic and heterotrophic microorganisms.

Trace metals and primary production

As mentioned above, phytoplankton require trace metals as cofactors for some enzymes and for components of electron-transfer chains in mitochondria and chloroplasts. These requirements are reflected in the vertical distributions of essential metals (e.g. zinc and iron) in the ocean. Most essential metals are depleted at the surface and increase with depth (Fig. 3.16).

Most trace metals are present at pico- to nanomolar levels in surface seawater, whereas cellular concentrations in phytoplankton are in the micromolar range. Many of the

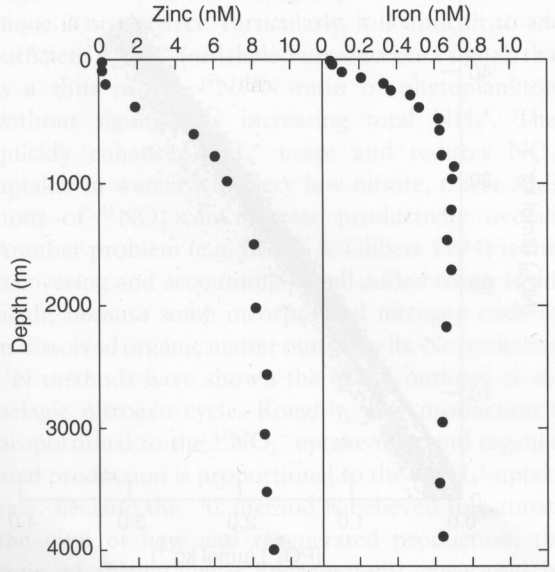

Fig. 3.16 Vertical profiles of dissolved zinc at (32°41′N, 144°59′W) and iron at (50°N, 145°W) in the North Pacific Ocean. (After Bruland 1980, and Martin *et al.* 1989.)

trace metals are present in non-reactive chemical forms; they are bound to strong metal chelators. This complicates determination of the mechanism and kinetics of phytoplankton uptake, but some progress has been made. Four types of uptake systems have been identified for iron: (i) transporters specific to particular iron compounds, e.g. Fe-citrate and siderophores; (ii) FeII transporters that oxidize FeII as it is transferred across the membrane, e.g. oxidase–permease complexes; (iii) FeIII reductases; and (iv) unchelated FeIII transporters (Morel *et al.* 2008). These uptake systems can be studied in cultured phytoplankton, but it is extremely difficult to determine which systems are most important in natural populations of phytoplankton in seawater.

Due to the supply of iron from terrestrial environments, iron concentrations can be 100 to 1000 times higher in coastal than in oceanic waters. Early studies (Brand 1991; Sunda *et al.* 1991; see also Fig. 1.1) with cultured phytoplankton showed that the iron requirements of oceanic and neritic phytoplankton reflect this difference and that oceanic clones are able to grow at much lower iron concentration than their coastal counter parts. Sunda and Huntsman (1995) extended this work by studying iron-uptake rates of three coastal and three oceanic phytoplankton species ranging in diameter from 3 to 13 μm. They found that uptake rates normalized to cell surface area were similar in all six species. This similarity is explained if evolutionary pressures have driven all species to develop uptake at the maximum limits imposed by diffusion and ligand exchange rates. Thus, oceanic species have been forced to reduce their cell size and/or reduce their growth requirement for iron. They also found that coastal diatoms appear to accumulate 20–30 times more iron than is required to meet their metabolic needs, compared with a two- to three-fold excess uptake in a coastal dinoflagellate and an oceanic coccolithophore.

The relative requirements for trace metals to support phytoplankton growth have been determined by growing phytoplankton in cultures and then analyzing their metal and phosphorus content by high-resolution, inductively coupled, plasma mass spectrometry (HR–ICPMS) (Ho *et al.* 2003). Results for 15 different species can be presented as an expanded Redfield formula for those elements known to be required for growth:

$$C_{124}N_{16}P_1S_{1.3}\ K_{1.7}Mg_{0.56}Ca_{0.5}$$
$$(Fe_{7.5}Mn_{3.8}Zn_{0.80}Cu_{0.38}Co_{0.19}Mo_{0.03})/1000.$$

Although ratios varied among the species examined, in general: Fe > Mn > Zn > Cu > Co > Mo. The high cell quotas for Fe are due to its abundance and major role in electron transport in the photosynthetic systems. Over 90% of the phytoplankton metabolic requirement for Fe is for photosynthesis, with two Fe atoms/PSII

complex, 12 Fe atoms/PSI complex, and six Fe atoms/(Cyt) b_6f complex.

Falkowski *et al.* (2004) suggested that cyanobacteria and the green plastid algae (those derived from a primary endosymbiosis of a cyanobacterium; see Plate 2.1) evolved first in the Proterozoic ocean (2500 to 542 million years ago). At that time, oceanic Fe, Zn, and Cu concentrations were high, so the green plastid algae consequently have higher Fe, Zn, and Cu cell quotas than the later evolved "red plastid" algae (those derived from a secondary endosybiosis of a rhodophyte, see Fig. 2.1). The red plastid algae, including prymnesiophytes, diatoms, and some dinoflagellates, have higher Mn, Co, and Cd cell quotas than the green plastid algae. Quigg *et al.* (2003) attribute the high iron quota of "green plastid" algae to the high PSI : PSII ratio in this group, while the "red plastid" algae have a low iron requirement due to a low PSI : PSII ratio. For present-day conditions, however, the major differences in iron cell quotas are apparent in the comparison of oceanic and coastal phytoplankton, rather than between phylogenetic groups. For example, Strzepek and Harrison (2004) showed that the oceanic diatom *Thalassiosira oceanica* minimizes its iron demand by greatly reducing its level of PSI relative to PSII, yielding a PSI : PSII ratio of 0.1 compared with the PSI : PSII ratio of 0.5 found in the coastal diatom *Thalassiosira weissflogii*. Thus, the oceanic diatom has adapted to low iron by reducing its iron requirement, but at the cost of no longer being able to respond quickly to wide variations in light intensity using PSI.

Marchetti *et al.* (2006a & b) compared iron cell quotas for different diatom species grown in Fe-replete and low-Fe culture media. Oceanic isolates of *Pseudonitzschia*, a genus often found at sea during iron-enrichment experiments, accumulated 60 times more iron than needed for growth at low iron concentrations, while coastal isolates accumulated 25 times more than needed. Such accumulation ratios for oceanic and coastal isolates of *Thalassiosira* were 14 and 10 respectively.

Finkel *et al.* (2006) conducted a more comprehensive study to compare the genetic (phylogenetic) versus environmental (phenotypic) variations in iron demands of different phytoplankton. They examined Fe, Mn, Zn, Cu, Co, and Mo levels in five phytoplankton species grown at five different light intensities. Metal to phosphorus ratios varied by one to three orders of magnitude. The Fe : P for all species examined ranged from 2 to 1000 Fe : P (mmol : mol). Diatoms and cyanobacteria showed the widest ranges of Fe : P 2–251 and 7–1053, respectively, while the dinoflagellate and prasinophyte had much narrower ranges of 18–359 and 9–52 respectively. The results show that variations in light levels had as great or greater effect on metal : P ratios, than group or species differences.

Iron and light interactively affect the cell composition, the rates of primary production, and the growth of marine phytoplankton. The efficiency of the iron-uptake mechanism; variations in iron requirements for PSI and PSII; and wide ranges in iron cell quotas, all suggest the importance of successfully competing for limited iron supplies. Experiments with laboratory cultures suggest some of the strategies used by different phytoplankton. Mackey *et al.* (2008) examined variations in photosynthetic electron flow in natural phytoplankton communities dominated by either *Synechococcus* or *Prochlorococcus* in high-light, low-nutrient environments. Both groups have oceanic clones with low PSI : PSII ratios, presumably an adaptation to low iron availability. Low levels of PSI restrict the electron flow from PSII to PSI and expose PSII to photo-damage. In these picoplankters, the cell prevents photodamage with plastoquinol terminal oxidase (PTOX), an enzyme downstream of PSII that uses electrons to reduce oxygen and regenerate water. This pathway decouples oxygen cycling from CO_2 fixation in photosynthesis, and appears to be widespread in oceanic surface layers.

Effects of temperature variation on primary productivity

Increased temperature affects phytoplankton growth as it does other metabolic processes: it makes the reactions proceed faster. Since many reactions with a variety of kinetics are involved in photosynthesis, there is no simple relation between either photosynthetic rate or growth rate and temperature. Most importantly, different species respond differently to temperature variation. Furthermore, temperature interacts with other factors such as nutrient availability to determine rates, so that the relationships can be complex. However, at an ecological level the effect of temperature is to set an overall upper limit on growth rates. A data compilation by Smayda (1976, 1980) of maximum cell division rates for many species (Fig. 3.17) shows increasing exponents over ranges of 10°C or more, and then, for most species, rather steep drop-offs above a thermal limit. Eppley (1972) plotted a scatter diagram from a similar data compilation of rates from batch cultures, but without distinguishing the species. He then fitted an upper envelope to the data, using an exponential equation. Actual μ_{max} values for individual species do not look much like the envelope. The higher points, especially below 10°C are mostly for diatoms, which have higher growth potential than other phytoplankton, when only internal physiological interactions (rates set by temperature) are limiting. Flagellates are mostly slower. Bissinger *et al.* (2008) analyzed a larger data-set, completed a thorough statistical analysis and proposed this modification of Eppley's equation:

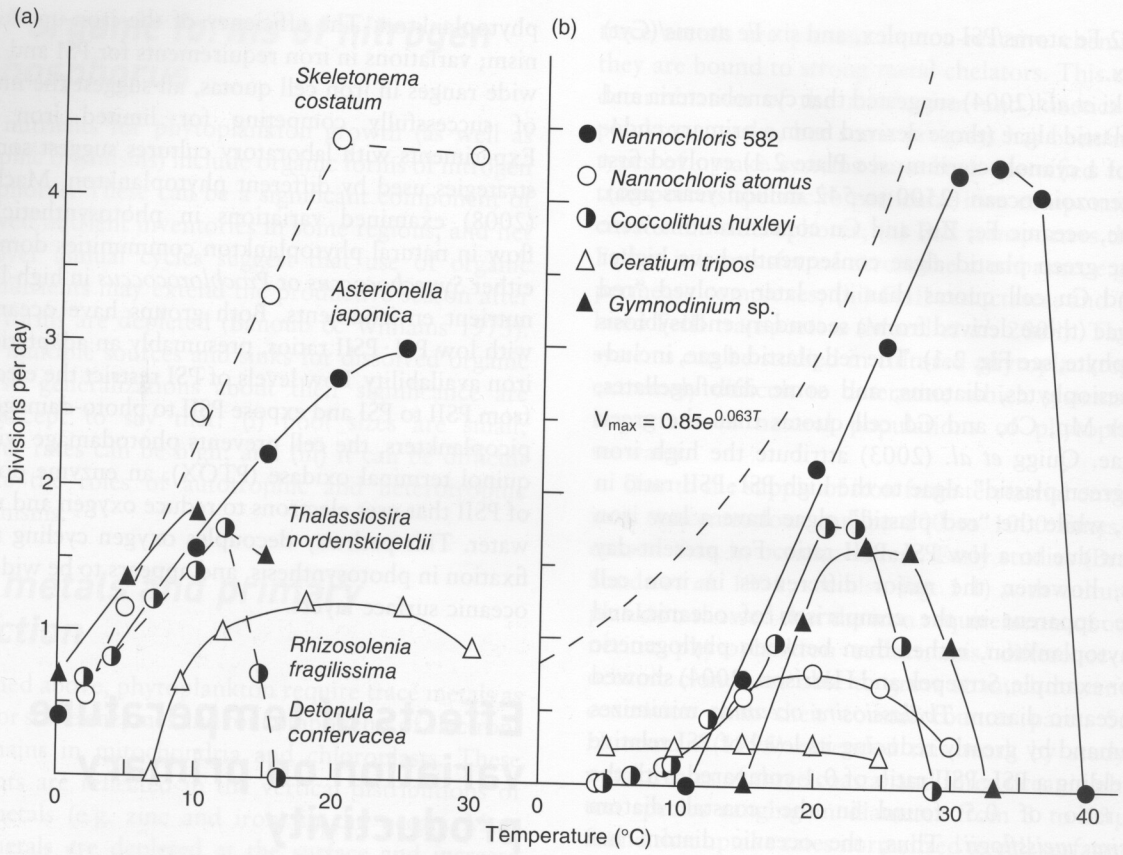

Fig. 3.17 Temperature effect on phytoplankton growth rate for several species: diatoms left, flagellates right. Dashed line on the right is the "Eppley curve", μ (doublings/day) = 0.85 exp(0.0637). (After Smayda 1976.)

$$\mu_{max} = 1.169 \exp^{(0.0631T)}.$$

which suggests that growth at lower temperatures may be up to 30% faster than estimated from the original Eppley equation (Fig. 3.18).

Goldman and Carpenter (1974) examined the temperature responses of several species in chemostats. They used an Arrhenius plot (Fig. 3.19) to present the data, and fitted an Arrhenius-type equation to it, rate = $f(1/T$ in °K). Their description of results for a number of species is:

$$\mu_{max} = (1.8 \times 10^{10}) \exp^{(-6842/T)}.$$

This curve is below that of Eppley, when that is plotted on the Arrhenius axes, but the actual quantitative difference is small (see also Goldman 1977). The difference obviously comes from Eppley's fitting of an upper envelope (which must be positioned subjectively) compared to the Goldman–Carpenter approach of fitting a relation to the central tendency of their data (probably more reliable). Both of these functions are commonly used in numerical models to characterize the response of phytoplankton to temperature.

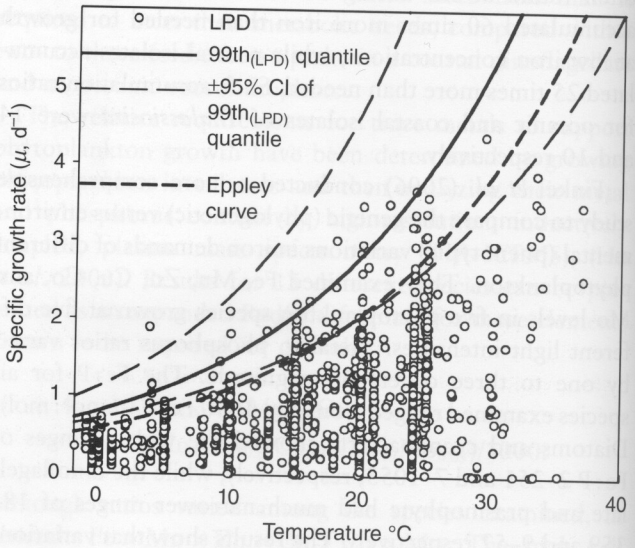

Fig. 3.18 Daily doubling rates of a wide variety of phytoplankton cultured at a range of temperatures. Fitted maximum rate curves are that due to Eppley (1972) and one fitted (with confidence limits) by Bissinger *et al.* (2008) to a larger set of species in the "Liverpool phytoplankton database" (LPD). (After Bissinger *et al.* 2008.)

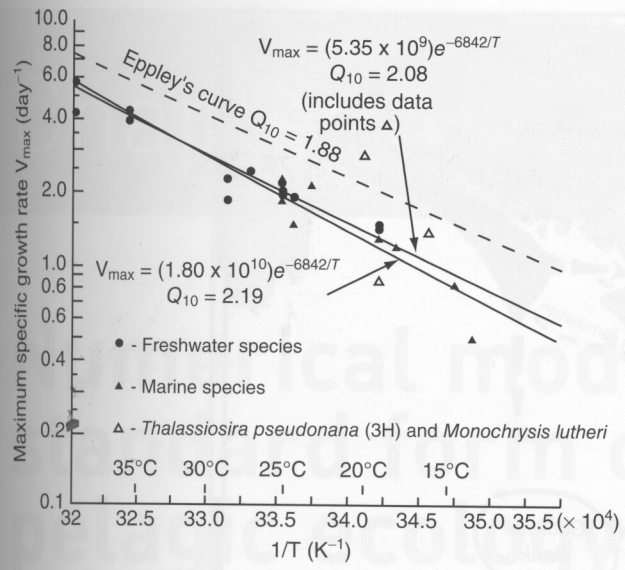

Fig. 3.19 An Arrhenius plot of V_{max} (nutrient and light saturated growth) vs. temperature. The form of the plot allows graphic determination of equation parameters. Data represented by points are from chemostat studies. (After Goldman & Carpenter 1974.)

Resting stages

Many diatoms and dinoflagellates form resting stages (cysts or spores) in response to unfavorable environmental conditions. Resting spores are more common in centric diatoms than in pennates (Hasle and Syvertsen 1997). Culture studies show that diatom resting stages can retain viability for at least two years. Field studies show that some benthic resting stages remain viable for only a few years, while others remain viable for decades (McQuoid & Hobson 1996; McQuoid *et al.* 2002). It is likely that these resting stages form the seed stock for pelagic phytoplankton blooms when they are resuspended from the sediment. Wetz *et al.* (2004) conducted experiments during the late winter to determine whether samples from the bottom boundary layer in coastal waters contained viable seed stocks that could serve to initiate a spring bloom. Growth occurred at light levels that were 40–50% of surface light, indicating that the resuspended cells could resume growth, but that winter mixing was deep enough to prevent growth.

Dinoflagellate cysts typically have a different cell wall from actively growing cells, and often require a period of cold and dark before being able to excyst. At the termination of a bloom, dinoflagellates (especially *Alexandrium* species) undergo sexual reproduction and the swimming zygotes form dormant cysts that can remain viable in the sediment for years. Recurrent toxic blooms in the Gulf of Maine have been a problem for a century or more. The main cyst seedbed is in the north-east part of the gulf near the mouth of the Bay of Fundy. One long-standing dilemma about these blooms is that the circulation patterns in the gulf are mainly to the west and south (Fig. 3.20) and should create, in effect, a one-way transport system with limited opportunity for cells to circulate back to the northeast. Anderson *et al.* (2005) and McGillicuddy *et al.* (2005) hypothesized a resolution based on models of the circulation patterns: cells accumulate in a retentive eddy near the mouth of the Bay of Fundy, allowing cysts to be deposited in that area to reseed future blooms. Cells that escape that retention zone into the eastern segment of the Maine Coastal Current bloom farther downstream and form a second seedbed offshore of the Androscoggin and Kennebec Rivers (Fig. 3.20). Germination of cysts in this second seedbed propagates the species farther along the Maine coast.

Cautions and future prospects

Phytoplankton ecologists have been a semi-independent subset among biological oceanographers. They have taken intense interest in factors controlling phytoplankton growth in the sea, and they have revealed many aspects of these relationships. However, several issues have become apparent. Cultured phytoplankton are not necessarily representative of the dominant phytoplankton in the ocean. The use of cultures inevitably involves unnatural conditions, including isolation of phytoplankton from their full set of natural associations. Production rate incubations disrupt normal grazing and regeneration processes. Thus, while light and nutrient conditions are important, phytoplankton stocks are as much controlled by grazing as by factors regulating cell growth. With exceptions like the onset of red tides, most of each day's phytoplankton growth is eaten *on the same day*. Increases such as spring blooms result from generally modest net differences between cellular multiplication and grazing. It is useful to examine phytoplankton in isolation, but the results must always be considered in light of the full set of interactions to which these small cells are subjected.

Molecular techniques and genomic analysis are elucidating both the phylogenetic relationships and previously unrecognized metabolic functions in the various phytoplankton groups. Genomic inventories suggest the existence of multiple enzymatic pathways for nutrient acquisition and metabolism, but do not indicate if and when these pathways are used. The challenge remaining is to combine these molecular and genomic techniques with *in vitro* and *in situ* experiments to determine key relationships of phytoplankton to both their physical–chemical environment and their co-existing microbes and zooplankton.

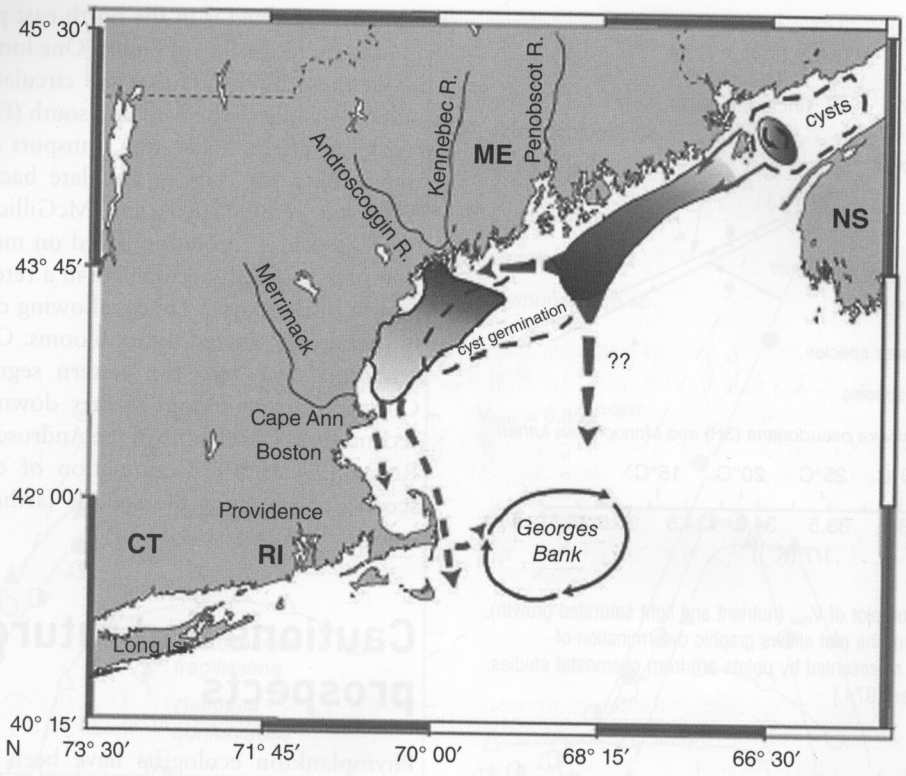

Fig. 3.20 Conceptual model of *A. fundyense* cysts and motile cell dynamics in the Gulf of Maine. Areas enclosed with dashed lines denote cyst seedbeds that provide inoculum cells. Major current systems are shown with shaded arrows. The shaded areas represent growth and transport of motile cells. (After Anderson *et al.* 2005.)

Ideally, we would like accurate estimations of primary production by phytoplankton and the subsequent use of the fixed carbon by other organisms. However, plankton communities are diverse. Several different organisms may serve similar functions, and a single organism can serve multiple functions. For example, *mixotrophs* have the capacity for both primary production and heterotrophic production (via use of dissolved organic material and/or phagotrophy of particulate organic material). This presents a problem in distinguishing between primary and secondary production processes. We will return to some of these complexities in Chapter 5 ("A Sea of Microbes") and Chapter 9 ("Pelagic Food Webs").